ANALYSIS OF PUMPING SCHEMES FOR THE EXTRACTION OF CONTAMINATED GROUNDWATER AT CAPE COD, MASSACHUSETTS, USING 3-D NUMERICAL MODELING

by

ENRIQUE J. LOPEZ-CALVA
B. S. Oceanography
Universidad Autónoma de Baja California, 1993

Submitted to the Department of Civil and Environmental Engineering
In Partial Fulfillment of the Requirements for the Degree of

MASTER OF ENGINEERING
IN CIVIL AND ENVIRONMENTAL ENGINEERING

at the

MASSACHUSETTS INSTITUTE OF TECHNOLOGY
June 1996

Signature of the Author _____

...ıal Engineering
May 10, 1996

Certified by _____

Lynn W. Gelhar
William E. Leonhard Professor of
Civil and Environmental Engineering
upervisor

Accepted by _____

Professor Joseph Sussman
Chairman, Departmental Committee on Graduate Studies

ANALYSIS OF PUMPING SCHEMES FOR THE EXTRACTION OF CONTAMINATED GROUNDWATER AT CAPE COD, MASSACHUSETTS, USING 3-D NUMERICAL MODELING

by

ENRIQUE J. LOPEZ-CALVA

Submitted to the Department of Civil and Environmental Engineering
On May 10, 1996
In Partial Fulfillment of the Requirements for the Degree of
Master of Engineering in Civil and Environmental Engineering

ABSTRACT

Past releases of hazardous materials at the Massachusetts Military Reservation have resulted in extensive contamination of the unconfined aquifer underlying western Cape Cod. Chemical Spill 4 is a plume of contaminants being contained by a pump and treat system. A well fence consisting of 13 extraction wells is currently operating at the downgradient edge of the plume. However, this pump and treat system was designed to as an interim remedial action to quickly respond to the plume migrating off site. A final remedial plan must be formulated to completely clean up the groundwater.

The objectives of this study were to evaluate the flexibility of the existing well fence, in terms of the different ways in which it can be operated to respond to different field conditions, and predict and alternative pumping scheme which can reduce operation and maintenance costs.

A three-dimensional, finite-element computer model was developed to get a comprehensive understanding of the groundwater flow and contaminant transport in the aquifer. The flow model was coupled with particle tracking simulations, to analyze capture curve geometry and analyze effectiveness of different pumping schemes. Cross-sectional area of the capture curves were reviewed, and compared to the cross-sectional area of the CS-4 plume. The effectiveness criteria were the complete capture of the plume, the minimum amount of clean water removed from the aquifer and a low pumping rate.

Simulations of pumping schemes based on eight and seven wells pumping 140 gpm, resulted in capture curves very similar to the capture curve of the existing well fence. The simulation of this existing well fence resulted in the capture of the plume in an efficient way. When the assumption of one well out of operation was made, and the simulation run, a capture zone with the same geometry as the one from the 13 wells was obtained, by redistributing the pumping rates. Greater dimensions of the capture zone, up to 50% bigger capture zone, was obtained increasing the overall pumping rate in the 13 well fence. The capture of particles from the lower part of the aquifer, however, was not easily attained.

The findings in this study indicate that a seven well system pumping an overall rate of 140 gpm would be an effective alternative pumping scheme for the containment of CS-4. The operation and maintenance costs would presumably be reduced and the capture of the plume

would still be attained. However, to provide the necessary hydraulic control for the containment of the CS-4 plume, the 13 well fence currently operating at the MMR proves to be effective and flexible, in terms of its response to different field situations. Modifications to this pumping scheme will need to consider well spacing, well screen depth and pumping rate distribution.

Thesis Supervisor: Dr. Lynn W. Gelhar

Title: William E. Leonhard Professor of Civil and Environmental Engineering

ACKNOWLEDGMENTS

Coming from a different country, I often feel awkward expressing my gratitude. Sometimes too little, sometimes too much, sometimes untimely, sometimes timely but not gracefully. Since this time I have the opportunity to write it down, I hope I can do a better job.

I must thank my thesis advisor, Professor Lynn Gelhar for his constant and patient input and guidance. Dr. Gelhar possesses the rare property of being both, extremely intelligent and extremely kind, and I am one of many who has benefited from this rare property.

Special thanks to Professor David Marks for all his help, and for making sure that I was doing OK. I must thank Ed Pesce from the Installation Restoration Program and Denis LeBlanc from US Geological Survey for sharing their time and knowledge. I also wish to thank the Consejo Nacional de Ciencia y Tecnología de México, the institution that sponsored me. I would not be finishing this program and this thesis without their financial support.

I should emphasize that this thesis constitutes a part of a much larger project, developed as part of the Master of Engineering program. This thesis could never have been completed without my team mates: Christine Picazo, Alberto Lázaro, Crist Khachikian, Donald Tillman and Pete Skiadas. This was a great team. I would not mind writing another thesis with them.

I am grateful to Bruce Jacobs for lending his expertise and teaching me all I know about DynSystem in such a friendly and patient way. Speaking about the code, I would like to thank all my modeling colleagues in the M. Eng: Alberto Lázaro, Vanessa Riva, Mitsos Triantopoulos, Dan Alden and Kishan Amarasekera. Fortunately we learnt how to help each other when something was going wrong with the computer (they say that when the blind leads the blind, both end up in the ditch, but who wants to be in the ditch alone?). All the M. Eng. students enriched me in some way or another, I thank them all.

My deepest and warmest gratitude goes to Maga, Maru and Salvador, who happen not only to be the emotional support that every MIT student needs (I guess every person does), but also and more remarkably, the best friends one can have.

It goes without saying that I would not be here without my family. I owe them more than any few sentences on a page like this can express.

TABLE OF CONTENTS

LIST OF FIGURES

LIST OF TABLES

1. INTRODUCTION

1.1 Problem Definition

Past releases of hazardous materials at the Massachusetts Military Reservation (MMR), have resulted in extensive contamination of the unconfined aquifer underlying western Cape Cod. In this aquifer, which supplies potable water to the residents of the area, various plumes of different contaminants have been detected. One such plume of contaminants, termed Chemical Spill 4 (CS-4), is currently being contained, under the Department of Defense Installation Restoration Program. At present, a pump and treat system has been installed to prevent the advancement of the plume. Contaminated water is extracted at the toe of the plume, treated to reduce the contaminant concentrations to federal maximum contaminant levels and then returned to the aquifer. However, this pump and treat system was designed to as an interim remedial action to quickly respond to the plume migrating off site. A final remedial plan must be formulated to completely clean up the groundwater.

1.2 Objectives

Complete comprehension of the natural flow and transport conditions of water and contaminants in the Cape Cod aquifer is the first objective. To accomplish this, it is necessary to establish a firm understanding of the hydrology, geology, hydrogeology, and geochemistry of the aquifer. Using inferred, calculated and predicted values for the above-mentioned factors, a computer model is established that adequately represents the existing conditions.

The second overall objective, once the flow field is characterized, is to develop a final remediation method, based on an alternative pump and treat system and an in situ bioremediation process.

In particular, the model developed is used to analyze the geometry of the capture zones resulting from different pumping scenarios and:

1. Predict an effective pumping scheme for the extraction of the contaminated water, and
2. Analyze the flexibility of the existing well fence, in terms of the way it can be used to respond to different field conditions.

1.3 Scope

This study covers the technical aspects of the current situation of the CS-4 plume at the MMR, and describes new clean-up strategies based on combinations of bioremediation and alternative pump and treat schemes.

Chapter 2 describes the site. General geographical background information is provided as well as the history of the activities at MMR. These data are needed to understand the extent of the groundwater contamination.

Section 2.2 covers the site characterization. The presented physical properties of the site are based on the review of reports of previous studies at the area as part of the Installation Restoration Program, and on studies of the site not necessarily related to the contamination problem. This site characterization is needed to develop the conceptual model, assign hydrogeologic properties to the area of the aquifer modeled, and help in the model calibration. Included in this section are results regarding the sorption behavior of the contaminants, which were found by conducting laboratory studies.

The current situation at the CS-4 site is presented inSection 2.3, including an overview of the plume extent and a description of the existing interim remedial action.

In Chapter 3, the basis of groundwater modeling is presented. Section 3.1 presents the problem definition of this part of the study, corresponding to the pumping schemes. This particularization of the research problem is necessary to understand the specific objectives, the findings and their relevance to the overall problem.

In order to develop any groundwater model, a conceptual model is needed. The conceptual model for this study is described in Section 3.2. The approach is discussed

and the set of assumptions presented. Delimitation of the modeled area, discretization and hydraulic boundaries are described.

Based on the conceptual model, a methodology was designed and followed to assign aquifer properties, calibrate the model, and simulate pumping schemes. This methods are described in detail in Section 3.3. This description is indispensable to fully understand the results from the model and their meaning. In particular, Section 3.3.2, which describes the methods followed for pumping schemes simulations, is important to interpret the results appropriately.

Chapter 4 presents the pumping schemes analysis. General observations are presented about the different geometry of the capture zones, according to different pumping scenarios. This previous analysis is needed as a basis to discuss the flexibility of the well fence, and the different ways to obtain effective capture zones. Results of the various simulations are presented and discussed.

Chapter 5 presents the conclusions about the pumping schemes analysis, which are drawn from the findings of the previous chapters.

In order to cover the different aspects of the overall problem of designing a final remedial design, different tasks were formulated and examined in depth, as part of the group project. Appendix A summarizes the findings resulting from the following studies:

Modeling the CS-4 plume under natural flow conditions the sequential anaerobic-aerobic in situ biodegradation, and the design and implementation considerations are presented; the economical benefits of combining zero-valent iron technology with the GAC as an additional remedial option; and risk assessment.

2. SITE DESCRIPTION

2.1 General Description

2.1.1 Location

Cape Cod is located in the southeastern most point of the Commonwealth of Massachusetts (Fig. 2.1). It is surrounded by Cape Cod Bay on the north, Buzzards Bay on the west, Nantucket Sound to the south, and the Atlantic Ocean to the east. Cape Cod, a peninsula, is separated from the rest of Massachusetts by the man-made Cape Cod Canal.

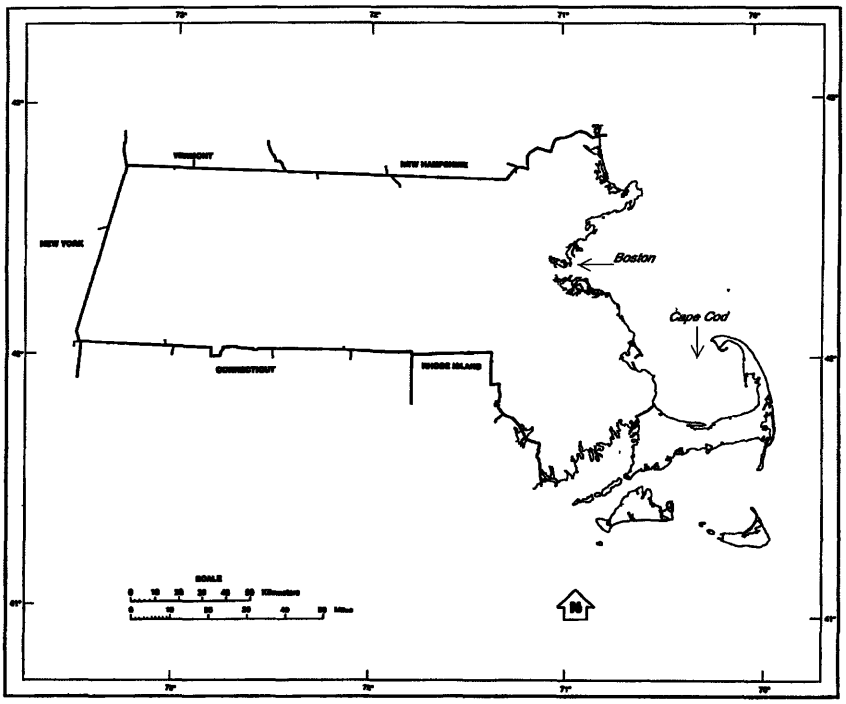

Figure 2.1. Map of the Commonwealth of Massachusetts

The Massachusetts Military Reservation (MMR is situated in the northern part of western Cape Cod (Fig. 2.2). The MMR, previously known as the Otis Air Force Base, occupies an area of approximately 22,000 acres (30 square miles).

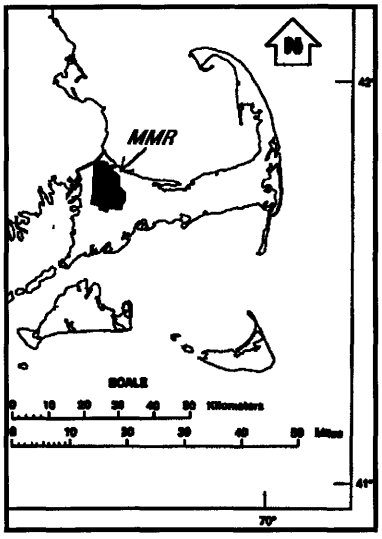

Figure 2.2. Location of MMR

2.1.2 Geopolitics and Demographics

Geopolitically, Cape Cod is located in Barnstable County, and is divided into 15 distinct municipalities: all of these municipalities (townships) have their own individual form of government and community organizations. The reservation is bordered by four townships: to the west by Bourne, to the east by Sandwich, to the south by Falmouth, and to the southeast by Mashpee.

The population of Cape Cod fluctuates with the season. In 1990, U.S. Census Bureau (USCB) determined the number of year-round residents to be 186,605 (Massachusetts Executive Office of Environmental Affairs, 1994). It is estimated that the number of Cape residents triples from winter to summer, topping a half million with the influx of summer residents and visitors (Cape Cod Commission, 1996). The county's median age in 1990 was 39.5 years (Cape Cod Commission, 1996). Age distribution studies conducted by the USCB, conclude that 22% of the Cape's residents are aged 65 and over, the highest percentage of this age group in any county in Massachusetts (Cape Cod Commission, 1996). Population growth studies estimate the year-round population of Cape Cod to increase 23% by the year 2020 (Massachusetts Executive Office of Environmental Affairs, 1994).

2.1.3 Natural Resources

Cape Cod is characterized by its richness of natural resources. Ponds, rivers, wetlands and forests provide habitat to various species of flora and fauna. Many of the Cape's ponds and coastal streams serve as spawning and feeding grounds for many species of fish. The Crane Wildlife Management Area, located south of the MMR in western Cape Cod, is home to many species of birds and animals. In addition, throughout the Cape there are seven Areas of Critical Environmental Concern (ACEC) as defined by the Commonwealth of Massachusetts. These were established as areas of highly significant environmental resources and protected because of their central importance to the welfare, safety, and pleasure of all citizens.

2.1.4 Land and Water Use

The majority of the land in Cape Cod covered by forests or is "open land". Twenty-five percent of the land is residential, while only less than 1% of the land is used for agriculture or pasture (Cape Cod Commission, 1996).

Water covers over 4% of the surface area of Cape Cod. This water is distributed among wetlands, kettle hole ponds, cranberry bogs, and rivers. Nevertheless, all 15 communities meet their public supply needs with groundwater. The township of Falmouth is the only municipality that uses some surface water (from the Long Pond Reservoir) as a drinking water source

Water demand in the Cape follows the same seasonal variations as population. Water work agencies are called to supply twice as much water during the summer months (June through August) than during the off-season (September through May). The highest monthly average daily demand (ADD) in 1990 was in July when 34.98 mgd were used. The lowest monthly ADD was in February with 14.03 mgd (Water Resources of Cape Cod, 1994). The towns of Falmouth and Yarmouth have the highest demand for water, with a combined percentage of almost 30% of the Cape's total water demand (Massachusetts Executive Office of Environmental Affairs, 1994).

Agriculture also constitutes a part of the water use in Cape Cod. Cranberry cultivation is an important part of the economy of the Cape and a water intensive activity.

The fishing industry also provides a boost to the Cape's economy. Tourism accounts for a substantial part of the Cape's economy and therefore surface water quality is important for recreational purposes such as boating, swimming, and fishing.

2.1.5 MMR Setting and History

The MMR has been used for military purposes as early as 1911. From 1911 to 1935, the Massachusetts National Guard periodically camped, conducted maneuvers, and weapons training in the Shawme Crowell State Forest. In 1935, the Commonwealth of Massachusetts purchased the area and established permanent training facilities. Most of the activity at the MMR has occurred after 1935, including operations by the U.S. Army, U.S. Navy, U.S. Air Force, U.S. Coast Guard, Massachusetts Army National Guard, Air National Guard, and the Veterans Administration.

The majority of the activities consisted of mechanized army training and maneuvers as well as military aircraft operations. These operations inevitably included the maintenance and support of military vehicles and aircraft as well. The level of activity has greatly varied over the MMR operational years. The onset of World War II and the demobilization period following the war (1940-1946) were the periods of most intensive army activity. The period from 1955 to 1973 saw the most intensive aircraft operations. Today, both army training and aircraft activity continue at the MMR, along with U.S. Coast Guard activities. However, the greatest potential for the release of contaminants into the environment was between 1940 and 1973 (E.C. Jordan, 1989a). Wastes generated from these activities include oils, solvents, antifreeze, battery electrolytes, paint, waste fuels, transformers, and electrical equipment (E.C. Jordan, 1989b).

2.2 Site Geology and Hydrogeology

2.2.1 Geology

The geology of western Cape Cod is composed predominantly by glacial sediments deposited during the Wisconsin Period (7,000 to 85,000 years ago) (E.C.

Jordan, 1989b). The three predominant geologic formations of the western Cape are: the Sandwich Moraine (SM), the Buzzards Bay Moraine (BBM), and the Mashpee Pitted Plain (MPP). The two moraines were deposited by the glacier along the northern and western edges of western Cape Cod. Between the two moraines lies a broad outwash plain, known as the which is composed of well sorted, fine to coarse-grained sands. At the base of unconsolidated sediments (below the MPP), fine grained, glaciolacustrine sediment and basal till are present.

Both the outwash and moraines have relatively uniform characteristics at the regional scale, even though they contain some local variability. The sediments are stratified and thus the hydraulic conductivities are anisotropic. The MPP is more permeable and has a more uniform grain size distribution than the moraines.

The total thickness of the unconsolidated sediments (i.e., moraine, outwash, lacustrine, and basal till) is estimated to increase from approximately 175 feet near the Cape Cod Canal in the northwest to approximately 325 feet in its thickest portion in the BBM; it then decreases to 250 feet near Nantucket Sound in south. The thickness of the MPP outwash sediments ranges from approximately 225 feet near the moraines, to approximately 100 feet near shore of Nantucket Sound (E.C. Jordan, 1989a).

2.2.2 Hydrology

Cape Cod's temperate climate produces an average annual precipitation of about 48 inches, widely distributed throughout the year. High permeability sands and low topographic gradient, minimize the potential for runoff and erosion, and thus recharge values have been reported in the range of 17 to 23 inches/year (LeBlanc et al., 1986). Consequently, a large fraction of water that precipitates will migrate to the subsurface. This creates a high probability of contaminant transport from the surface to the groundwater.

Beneath western Cape Cod lies a single groundwater system (from the Cape Cod Canal to Barnstable and Hyannis) which the U.S. Environmental Protection Agency (EPA) has designated it as a sole source aquifer. This aquifer is unconfined and its only form of natural recharge is by infiltration from precipitation. The highest point of the

water table (the top of the groundwater mound) is located beneath the northern portion of the MMR. In general, groundwater flows radially outward from this mound and ultimately discharges to the ocean.

Kettle hole ponds, depressions of the land surface below the water table, are common on the MPP. These ponds influence the groundwater flow on a regional scale. Streams, wetlands and cranberry bogs serve as drainage to some of these ponds and as discharge to the groundwater, and thus comprise the rest of the hydrology of the western cape. Figure 2.3 shows some hydrologic features of western Cape Cod.

2.2.3 Hydrogeology

The geology and hydrology of western Cape Cod define the hydrogeologic characteristics of the aquifer. General information on about the geology and hydrology of Cape Cod can be found in the works by Oldale (1982), Oldale and Barlow (1987), Guswa and LeBlanc (1985), and LeBlanc et al. (1986). This section summarizes the data on the major aquifer properties measured throughout the area. Variability of these values may be due not only to natural heterogeneities of the soil, but also to differences in measuring techniques and data analysis (E.C. Jordan, 1989a).

Hydraulic Conductivity

Throughout the western Cape, there appears to be a general trend of decreasing conductivity from north to south and from the surface to the bedrock. The conductivity of the western cape has been studied extensively. Table 2.1 shows a summary of the hydraulic conductivity values reported in the literature. Geologic variability within the outwash suggests that some variability in hydraulic conductivity is likely. Nonetheless, the maximum and minimum values reported are probably biased by the analytical method or exhibit a small-scale geologic heterogeneity. An value of 380 ft/d (obtained from the Ashumet Valley pump tests and corroborated by the tracer test south of the MMR) has been accepted as a representative value of average hydraulic conductivity of the MPP outwash sands (E.C. Jordan, 1989a).

Table 2.1. Estimates of hydraulic conductivity of stratified drift, as determined from analysis of aquifer tests, Cape Cod Basin, Massachusetts. (Adapted from Masterson and Barlow, 1994).

Predominant grain size of tested interval	Latitude ° " '	Longitude ° " '	Horizontal hydraulic conductivity (ft/day)	Anisotropy ratio	Source of data
Fine sand and silt	41 36 06	70 30 29	40	50:1	Barlow and Hess (1993)
Fine sand	41 40 00	70 14 72	160	30:1	Barlow (1994)
Fine to medium sand	41 37 03	70 33 00	380	5:1-3:1	LeBlanc, et al. (1988)
Fine to coarse sand and gravel	41 40 10	70 13 53	220	10:1	Barlow (1994)
Medium to coarse sand and gravel	41 45 16	69 59 39	300	> 10:1	Guswa and LeBlanc (1985)

Anisotropy Ratio

The ratio of horizontal to vertical hydraulic conductivities (K_h/K_v) has been studied along with some of the hydraulic conductivity tests. Values of anisotropy ratio for different studies are reported in Table 2.1. Typical anisotropy values range from 10:1 to 3:1.

Porosity

Measured values of porosity range from 0.20 to 0.42. Effective porosity of the outwash is estimated from a tracer test (Garabedian et al., 1988; LeBlanc et al., 1991) to be about 0.39.

Hydraulic Gradient

The hydraulic gradient will be affected by the variations in water table elevations. These typically fluctuate about 1 m because of seasonal variations in precipitation and recharge. During the period of a tracer test (22 months), the hydraulic gradient in the

study area (Ashumet Valley) varied in magnitude from 0.0014 to 0.0020. Vertical hydraulic gradients measured during this test were negligible except near the ponds (LeBlanc et al., 1991).

Chemistry of the Water

The properties of the chemicals of particular interest to the bioremediation design are shown Table 2.2 (E.C. Jordan, 1990). The dissolved oxygen values vary with depth. The values reported are for the depths of interest (depth < 100 ft below water table). The concentration of metals is also of particular interest since high concentrations can have a detrimental/toxic effect to microbial growth. The concentration of metals tested for at CS-4 , however, are negligible.

Table 2.2. Groundwater properties

Property	Value
Dissolved oxygen (mg/L)	5.0-10.0
Nitrate (mg/L)	0-1.8
pH	5-7
Temperature	10° C

Equilibrium Sorption

Sorption of contaminants by aquifer solid matrices significantly effects their fate and transport. The bioavailability of contaminants can be reduced considerably because of sorptive uptake. Also, pump and treat times can be prolonged substantially because of a continuous feeding of contaminants to the aquifer by the sorbed species. Another effect of sorption is to alter the dispersive behavior of contaminants. While sorption acts to reduce the hydrodynamic dispersion of any one contaminant, it acts to enhance its longitudinal macrodispersivity.

One way to quantify all of these effects is to use equilibrium sorption distribution coefficients to calculated retardation factors. Laboratory batch tests are setup to

determine distribution coefficients. The depth-averaged retardation factors calculated for the contaminants of interest are listed in Table 2.3 (see Appendix A).

Table 2.3. Effective retardation factors

Compound	R_{eff}
DCE	1.04
TCE	1.10
PCE	1.25

2.3 Current Situation

2.3.1 Interim Remedial Action and Objectives for Final Remedy

The existing remedial action was designed as an interim system, with the objective of contain the plume against further migration. This is achieved by placing pumping wells at the plume toe and treating the extracted water (see Figure 2.3).

In contrast, the final remedial action will address the overall, long-term objectives for the CS-4 Groundwater Operable Unit which are as follows (ABB Environmental Services, 1992b):

- Reduce the potential risk associated with ingestion of contaminated groundwater to acceptable levels.
- Protect uncontaminated groundwater and surface water for future use by minimizing the migration of contaminants.
- Reduce the time required for aquifer restoration.

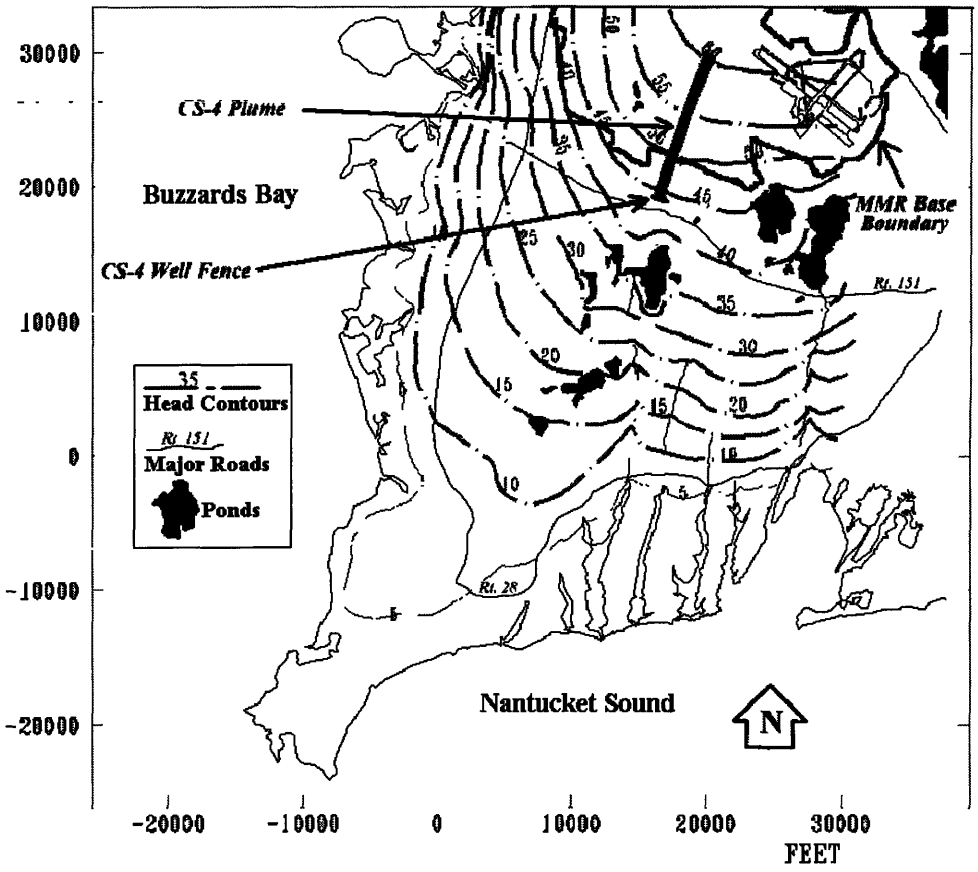

Figure 2.3. CS-4 plume and well-fence location

In terms of treatment objectives, the target levels for the treatment of the water are defined through the established Maximum Contaminant Levels (MCL). These apply to the contaminants of concern and are summarized in Table 2.4. Maximum measured concentrations, average concentrations within the plume, and an approximate frequency of detection are also given. It is important to realize that these values represent only an approximation, since their determination depends on a definition of the plume borders.

Although the existing remedial action is interim, its clean-up goals have to be consistent with the long-term goals. Therefore, the above target levels are applicable to the existing interim action.

Table 2.4. Contaminants of concern and treatment target level (Adapted from ABB Environmental Services, 1992b)

Contaminant of concern	Abbreviations	Maximum Concentration (ppb)	Average Concentration (ppb)	Frequency of detection	Target level (MCL) (ppb)
Tetrachloroethylene	PCE	62	18	14/20	5
Trichloroethylene	TCE	32	9.1	14/20	5
Total 1,2-Dichloroethylene	DCE	26	1.1	11/20	70
1,1,2,2- Tetrachloroethane	TCA	24	6.8	1/20	2*

* No Federal of Massachusetts limits existent. Therefore, a risk-based treatment level was proposed. This was calculated assuming a $1x10^{5}$ risk level and using the USEPA risk guidance for human health exposure scenarios.

2.3.2 Existing Remedial Action

The currently operating remediation system consists of the following components:

- Extraction of the contaminated groundwater at the leading edge of the plume by 13 adjacent extraction wells.
- Transport of the extracted water to the treatment facility near the southern boundary of the MMR.
- Treatment of the water with a Granular Activated Carbon (GAC) system.
- Discharge of the treated water back into the aquifer to an infiltration gallery next to the treatment facility.

The IRP well fence consist of 13 wells located at the toe of the plume, about 1000 ft north of Route 151. The wells are 60 feet apart, in a straight line (see Figure 2.4), covering a total distance of 720 ft. The well number 11 in the well fence, is not within the straight line defined by the rest of the wells, but located about 20 ft to the north of the line. Each well has a 15 feet screen, 8 inches in diameter. The bottom of the screen is

located at a depth of 140 ft. The overall pumping rate is 140 gpm. The wells located at the sides pump 15 gpm and the 11 wells in the middle pump 10 gpm. The water pumped to the treatment facility, treated with GAC, and discharged in an area near the treatment facility.

The treatment facility consists of two adsorber vessel in series filled with granular activated carbon. This system of two downflow, fixed-bed adsorbers in series is the simplest and most widely utilized design for groundwater treatment applications (Stenzel and Merz, 1989). Two vessels in series assures that the carbon in the first vessel is completely exhausted before it is replaced. thus contributing to the overall carbon efficiency. The removed carbon is then transported off-site for reactivation.

2.3.3 Plume Location

CS-4 plume is located in the southern part of MMR moving southward (see Figure 2.3 and 3.1). From field observations. the dimensions of the plume have been defined. According to E. C. Jordan (1990), CS-4 is 11,000 ft long, 800 ft wide and 50 ft thick.

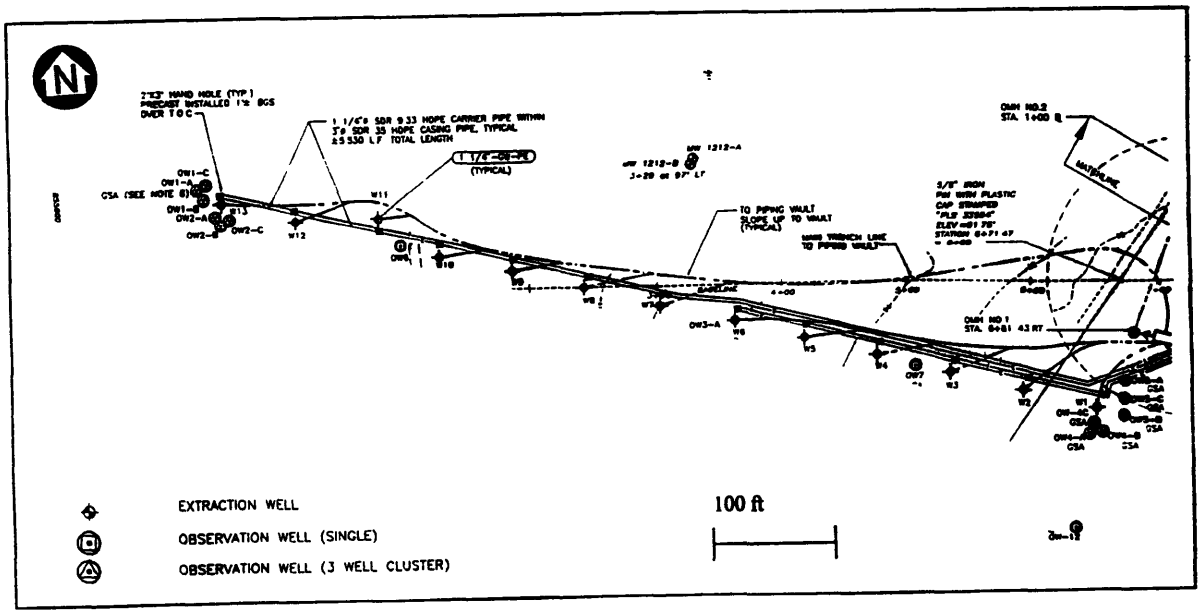

Figure 2.4. Well fence currently in operation at the downgradient edge of the CS-4 plume.

2.3.4 Other Technologies Considered

Looking at the technologies that were considered for an interim remedial technology gives a broader understanding of the reason for selecting the current pump and treat system. Of the 13 remedial technologies screened in the Feasibility Study (E.C. Jordan, 1990), five were selected and retained for detailed analysis. For further evaluation, they were compared against the following nine criteria:

- overall protection of human health and the environment
- compliance with ARARs (Applicable or Relevant and Appropriate Requirement)
- long-term effectiveness and permanence
- reduction of mobility, toxicity or volume through treatment
- short-term effectiveness
- implementability
- cost
- state acceptance
- community acceptance

The no action alternative served as a baseline for comparing various strategies (ABB Environmental Services, 1992a; E.C. Jordan, 1990). The selected carbon adsorption technology was evaluated against the following alternatives:

- air stripping followed by activated carbon
- UV oxidation
- spray aeration
- Otis Wastewater Treatment Plant

2.3.5 Performance of Current Remediation Scheme

Since the treatment facility started operating in November 1993, only minimal inflow concentrations (ABB 1996, personal communication) have been detected and treated.

Numerous scientific publications have raised serious concerns about the ability of existing pump and treat to restore contaminated groundwater to environmentally and

health-based sound conditions (Mackay and Cherry, 1989; Travis and Doty 1990; MacDonald and Kavanaugh, 1994). Other studies have shown that pump and treat in conjunction with other treatment technologies can restore aquifers effectively (Ahlfeld and Sawyer, 1990; Bartow and Davenport, 1995; Hoffman, 1993). However, there is a consensus that pump and treat is an effective means of controlling the plume migration.

In conclusion, the interim CS-4 pump and treat system seems to be an appropriate way to quickly respond to the plume migration. However, for the final CS-4 remedial system new ways of cleaning up the aquifer must be addressed. For this purpose, this study examined the feasibility of applying bioremediation and combining the existing carbon treatment with zero-valent iron technology.

3. GROUNDWATER MODELING

Groundwater flow and contaminant transport modeling can be used to conceptualize and study flow processes, recognize limitations on data, guide collection of new data, design remedial strategies and assist in problem evaluation. Therefore, groundwater modeling is a very important engineering tool to remediate a contaminated aquifer. This chapter describes the basis of the groundwater three-dimensional computer model used to analyze the "pump" portion of the pump and treat technology of this study.

3.1 Introduction

As mentioned in the previous section, the current remedial system, seems to be appropriate to contain the plume from further migration. Hoffman (1993), refers to pump and treat as the only groundwater cleanup technology that has successfully begun effective remediation of deep widespread groundwater contamination. However, this author also mentions that pump and treat has the disadvantages of being expensive to design, install and operate. Many other authors support this fact but also mention that pump and treat is the most efficient way to prevent contaminated groundwater migration, by providing the required hydraulic control (Hoffman, 1993; Ahlfeld and Sawyer, 1990; Gailey and Gorelik, 1993; Isherwood et al., 1993).

Due to this particular characteristics of pump and treat, it is still widely used but, at the same time, there is a great necessity of more carefully designed and operated systems, in order to minimize costs. Since pump and treat, as mentioned by Hoffman (1993), in all known cases must be maintained and operated for several years (decades), operation and maintenance cost are one of the most important factors to consider when designing a remedial system. Nyer (1994), mentions that in very long remedial projects, the savings in capital cost, may become insignificant in view of the overall cost of the remedial program. For these reasons, prediction of an alternative capture curve, based in fewer wells or lower pumping rate is one of the objectives of these work.

Cost-effectiveness involves, of course, the pumping schemes and the treatment technologies, as well as monitoring costs. This chapter, and the next one are focused only on the technical aspects of pumping schemes. Economic factors, although implicit and important, are mentioned but not emphasized. The treatment technology analysis is presented in Appendix A, and in this case, economic factors are carefully reviewed.

Different considerations are needed in the design of pumping schemes for the extraction of contaminated water. The first consideration is related to the main objective: to reduce concentrations of contaminants to an acceptable level (cleanup), or to protect the subsurface from further contamination (containment). Regardless of the main objective, general system components, according to Mercer and Skipp (1990), are:

- A set of goals or objectives
- Engineered components such as wells, pumps and treatment facility
- Operational rules and monitoring
- Termination criteria

Technical considerations are of course very important. Hydraulic conductivity, aquifer heterogeneity, sorption of the contaminants, immobile nonaqueous phase liquids, and many other factors are very important to consider in the pumping system design (Mercer and Skipp 1990).

The design of capture curves for contaminants can be made in a number of ways. Different approaches can be found in the literature. Analytical, semianalytical and numerical flow models are used with or without a particle tracking program to delineate the capture zones of wells. To define zones of hydraulic control and found proper well locations, simulation and optimization techniques have been used by several authors (Gorelick et al., 1993; Gailey and Gorelick, 1993; Ahlfeld and Sawyer, 1990). Groundwater velocity analysis (Heidari et al., 1987), three-dimensional simulations combined with mixed-integer programming (Sawyer et al., 1995), and analytical solutions (Javandel and Tsang, 1987; Yang et al., 1995) have also been developed, to define capture curves and well locations.

In this study, a three-dimensional finite-element numerical model, coupled with particle tracking is used to define the capture curves. The opportunity to evaluate a large number of alternatives combining different factors is one of the greatest advantages of the use of a three-dimensional numerical model to help in the design of remedial or containment systems. Some other advantages of this method over the analytical models discussed by Springer and Bair (1993) and Bair and Roadcap (1993), are the ability to account for complicated hydrogeologic settings and nonuniform characteristics, avoiding the conceptual errors due to assumptions common in analytical models.

Flexibility of the existing well fence

The remediation of a site is an active and continuous process. Monitoring contaminant concentrations and head values to determine hydraulic control, using monitoring wells is important in the remedial process. Some details in the remediation schemes can be modified according to monitoring results. In addition, evaluation of the performance of the extraction systems can be very important while remediating a site (Hoffman, 1993).

CS-4 plume is very particular in shape, as can be seen in Figure 3.1 since it is about 11,000 ft long and only 800 ft wide. This means that transverse dispersivity for this plume is extremely low, as explained below. Lázaro (1996), simulates the natural transport of this plume using a value of transverse dispersivity of 0.05 ft, and finds that, after traveling for thirty years and reaching the length of 11,000 ft, the plume would be wider than the plume reported by E. C. Jordan (1990). The value of 0.05 ft for transverse dispersivity used by Lázaro (1996) is among the lowest values presented by Gelhar et al. (1992), in a review of field-scale dispersion in aquifers. This author and Van der Kamp et al. (1994) explain how transverse dispersivity is caused primarily by the temporal variation in hydraulic gradient.

The explanation for a plume as narrow as CS-4 would be the existence of an extremely steady flow with minimum variations in the direction of hydraulic gradient. However, all these factors mentioned also suggest a review in site characterization. LeBlanc (1996) mentions that in many cases, the definition of the dimensions of a plume

keeps changing as we improve site characterization. For all these reasons one of the purposes of this study is to analyze the flexibility of the current pumping system, and the way it could be modified in response to a wider or deeper plume.

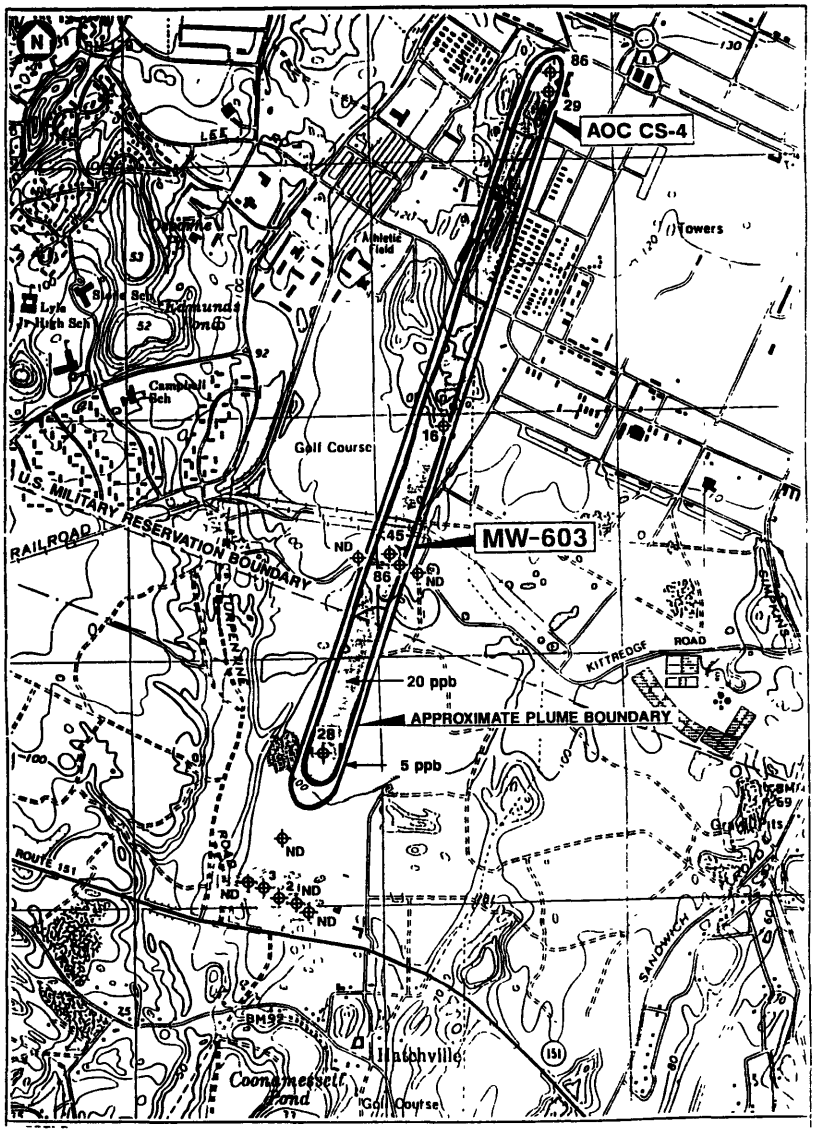

Figure 3.1. CS-4 Plume as reported by E. C. Jordan (1990) after the site characterization conducted under the Installation Restoration Program.

3.2 Conceptual model

The three-dimensional model is constructed using the finite-element modeling code DynSystem (Camp, Dresser & McKee, Inc, 1992). This numerical-modeling code has the flexibility to evaluate various extraction systems, and the ability to simulate most natural conditions observed in the area, in three dimensions. DynSystem is composed of three different codes:

1) DYNPLOT, which processes all input files (files containing information required to run simulations), and output files (files that can be plotted, presenting the results from simulations).

2) DYNFLOW, which processes all the input files to run flow simulations.

3) DYNTRACK , which uses input files containing information about solutes to simulate transport.

3.2.1 Approach

In order to accurately simulate the flow and transport under natural conditions, and qualify the effectiveness of a remedial system, the regional controlling factors must be incorporated into the modeling analysis. Considering the objectives of the project, the model is constructed in an area much greater than the area where CS-4 plume is located. A grid is built with a systematic and well structured refinement. The triangular elements defined by nodes are smaller in the areas of interest to meet numerical constraints and ensure accuracy. In addition, the requirements for vertical discretization are different for stress conditions (pumping) and non-stress conditions (natural flow). Vertical refinement of the grid is used after the model is calibrated, to run capture curve simulations. To run the pump-test simulation, a further modification to increase resolution is done using a regional to local interpolation into a much more discretized grid.

The model is developed according to some assumptions. Steady state conditions were assumed. Recharge due to precipitation is assumed to be uniform throughout the modeled area. Discharge from the aquifer is assumed to be due to natural downgradient flow (into the ocean), discharge into streams, and extraction from pumping wells.

3.2.2 Geometric boundaries

The model includes an area of approximately 51.5 mi^2 on the western Cape (southern part of the western Cape) sowed in Figure 3.2. The horizontal boundaries are defined by two non-flow boundaries and the ocean. The no-flow boundaries (flow lines) are defined by lines perpendicular to the head contours described by Savoie (1995).

The southern end of the model is Nantucket Sound, and Buzzards Bay is at the western end. The eastern boundary is a flow line directed towards Ashumet and Johns Ponds and down along the Childs River to salt water. The western shoreline of these two ponds delimit the modeled area, but the actual body of water is not included in the model. The northern boundary is another flow line originating at the same point of the eastern boundary (the upper-most point in the water table), and extending westward to Buzzards Bay (Figure 3.2).

The thickness of the modeled region is non-uniform, defined by the topographic characteristics of the Cape. As the aquifer is unconfined, the upper limit is the ground surface and the lower limit is the bedrock underlying the Cape Cod Area (Oldale, 1969).

3.2.3 Hydraulic Boundaries

Johns Pond, Ashumet Pond and Childs River are included in the model as boundary conditions. Coonamessett Pond is the most important surface water body within the modeled area because of its vicinity to the end of the CS-4 plume region. Since most of the pumping activity is going to occur in this region, this area is one of major interest. Other ponds included in the area of the model are Osborne, Deep, Edmonds, Crooked, Shallow, Round, Jenkins, Mares and Deer. The ponds are represented in the model as areas of very high hydraulic conductivity, and effective porosity equal to one. This is done to get negligible horizontal hydraulic gradients and to correctly represent the flat surfaces of these water bodies. Pumping wells are defined as nodes in the grid with negative flow.

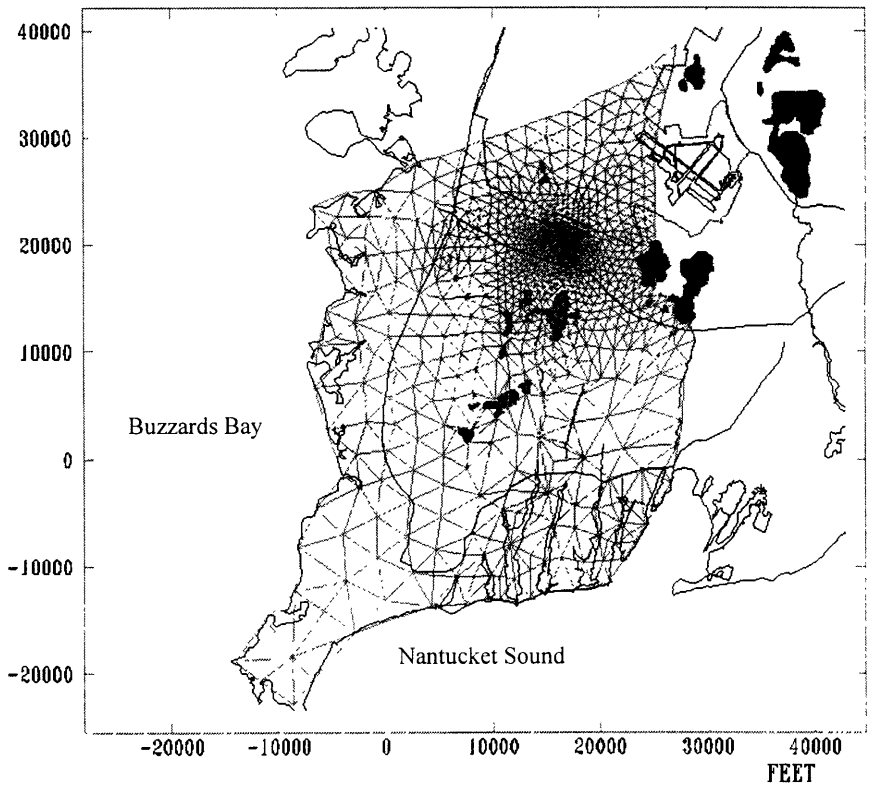

Figure 3.2. Horizontal discretization for the groundwater flow model. The grid includes more than 50 mi^2, divided into 2114 elements. Vertically, the grid is divided in 9 levels. Vertical discretization was increased to 15 levels for pumping simulations.

The saltwater-freshwater interface at the western and southern boundaries is constructed assuming hydrostatic conditions for the salt water, and defining an increase in hydraulic head with depth according to the density differences. Head is fixed at sea level in these boundaries. Fixed head is also used in the nodes corresponding to the boundaries of Johns and Ashumet ponds. The rivers are represented by nodes with a specified and well defined elevation.

The water table is represented by a special type of boundary condition, called rising water boundary condition. This same boundary condition is used at the surface of the ponds and rivers. A node with the rising water condition will have a value of head equal to or less than the elevation of the node.

3.2.4 Discretization

The grid contains 1194 nodes and 2314 elements, distributed horizontally. The vertical discretization consists of 9 levels, dividing the area into 8 different layers. Finer discretization is employed in the area of rapidly changing gradients due to pumping. This grid is used in the simulation of natural flow and transport. For the simulations of the different pumping schemes, however, the grid is modified to analyze hydraulic control due to pumping. Vertical resolution is increased up to 15 levels to better define the three dimensional capture curves (see Figure 3.2).

A local grid is constructed from interpolation of the regional grid to run a simulation of the pumping test carried out in the area in April of 1993, by ABB Environmental, Inc. (E. C. Jordan, 1990). This small local grid consists of 2090 elements defined by 1070 nodes, using 15 levels as the vertical discretization. This grid covers an area of about 1,540,000 ft^2.

3.3 METHODS

3.3.1 Natural Flow Model

Aquifer Properties Assignment

The area modeled is divided in two main lithologic entities: the glacial moraine, and the Mashpee Outwash. The Buzzards Bay Moraine is assumed to be composed of four different materials distributed vertically. The area of the outwash forming part of the model is divided into a northern and a southern areas in the horizontal, and in three different materials in the vertical direction, as indicated in Figure 3.3. Within these different facies, different materials are assigned according to the depositional model described by Masterson and Barlow (1994).

a) Hydraulic conductivity

Assignment of hydraulic conductivity is made following the approach of Masterson and Barlow (1994). This authors group the sediments in lithostratigraphic

units according to their depositional origin. As described in Section 2.2.1, within the Mashpee Outwash, sediments are coarse in the upper layers and fine in the lower layers. There is also a fining southward tendency. Hydraulic data from different studies in the area (Table 2.1) is used by these authors to determine approximate ranges of hydraulic conductivity for the lithostratigraphic units, based on the relation between lithology and hydraulic conductivity. Table 3.1 summarizes the distribution of the lithostratigraphic units, their lithology and hydraulic characteristics.

Table 3.1. Relation of lithology to hydraulic properties in western Cape Cod.

Depositional Origin	Lithostratigraphic unit	Lithology	Horizontal Hydraulic Conductivity (ft/day)	K_h / K_v
Glaciofluvial	Top-set beds			
	Proximal	Coarse sand and gravel	350	3:1
	Mid	Medium sand and gravel	290	3:1
	Distal	Fine sand and gravel	240	3:1
Glaciolacustrine	Fore-set beds			
(nearshore)	Proximal	Medium to coarse sand	280	3:1
	Mid	Fine to medium sand	200	5:1
	Distal	Fine sand	150	10:1
Glaciolacustrine	Bottom-set beds			
(offshore)	Proximal	Fine sand	150	10:1
	Mid	Fine sand and some silt	70	30:1
	Distal	Fine sand and silt	30	100:1
Glacial	Moraine	Sand, silt and clay; unsorted	30-150	10:1

Proximal: Sediments close to the moraines
Mid: Sediments in the central parts of the western Cape
Distal: Sediments away from the moraines

The values of hydraulic conductivity for fine sand and silt, fine sand, fine-medium sand, and medium-coarse sand and gravel (which are the four main materials found in the

Mashpee Pitted Plain) shown in Table 3.1 were used as a basis to create the input files of the model.

Anisotropy ratios are also defined, initially, based on the information presented by these authors. As in the case of horizontal hydraulic conductivity, anisotropy ratio is assigned to a particular type of sediment, which is then assumed to be homogeneously distributed along a well defined area in the Cape. The anisotropy ratio is an important calibration parameter for the transport model. Its value, initially based only on a literature review, is slightly modified according to the pumping test simulations and the transport model results (Appendix A). Initial anisotropy ratio values used in this model range from 3:1(coarse sands) to 30:1 (glacial moraine).

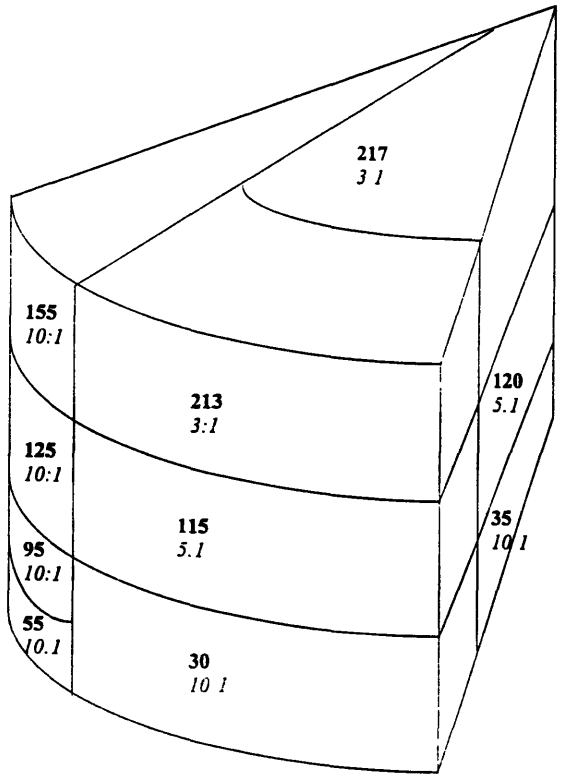

Figure 3.3. Conceptual distribution of horizontal hydraulic conductivity and anisotropy ratio in the western Cape Cod model

b) Recharge

Precipitation is the only source of fresh water to the Cape Cod groundwater-flow system. Actual recharge to the groundwater system is less, since some of the water either

evaporates or is transpired by plants. LeBlanc et al. (1986) and Barlow and Hess (1993), estimate that 45 to 48 per cent of the total precipitation, about 18 to 23 in/yr, recharges the aquifer. The value used in the flow model is 23 in/yr. During the flow calibration procedure, recharge is not treated as a calibration parameter and is maintained constant.

c) Hydraulic head

Initial values of hydraulic head are obtained from Savoie (1995). Water level data from more than 100 wells, distributed throughout the western Cape were measured in a period of two days. This data is the most representative head data available. Of the total number of well observations reported by this author, 106 wells were used to create the input file of the model. Data from a few wells located within the ponds or very close to them are discarded, since information about screen elevation is not available. These areas near the ponds are under vertical flow conditions and thus head is not constant with depth. Thus, specific screen elevation data is necessary to determine the actual head at that point. The vertical gradient is assumed to be negligible for the rest of the cape (predominantly horizontal flow was assumed). In order to assign a head value to each node in the grid, interpolation of the values is made using the capabilities of the code. This way a initial water table surface is obtained for the entire modeled area. Calibration, however is made with the original discrete points as targets, hence avoiding the possible interpolation bias.

d) Aquifer thickness

The lower limit of the modeled aquifer is considered the bedrock underlying Cape Cod. A thin layer of lacustrine sediments is present overlying bedrock. However, this material is not considered since its thickness becomes appreciable only in marginal portions of our modeled area. A topographic map of the basement surface (bedrock), is presented by Oldale (1969). From the seismic investigations made by this author, elevation contours of the bedrock were digitized and then interpolated to get the surface of the lower limit of the model.

e) Dispersivity

Garabedian et al. (1988) calculated dispersivities using the data obtained during the Ashumet Valley tracer test. The method of moments was used to interpret the data; which was regarded by Gelhar et al. (1992) as having a high degree of reliability. Values of dispersivity are summarized in Table 3.2 below.

Table 3.2. Dispersivity values of the Ashumet Valley Tracer Test (*Garabedian et al.*, 1988)

Dispersivity	Value
Longitudinal (A_L)	3.15 ft
Transverse, horizontal (A_T)	0.59 ft
Transverse, vertical (A_V)	0.005 ft

It must be noted that the values obtained by Garabedian et al. (1988) are for a source with dimensions of 16.4 x 16.4 x 3.3 ft and an overall test scale of 820 ft. In the case of the CS-4 site, the dimensions of the source (about 1050 x 450 x 50 ft) and the test scale (about 11,000 ft) are larger. Rajaram and Gelhar (1995) conclude that dispersivities for transport over large scales are significantly influenced by the source dimensions. Using their methods, the longitudinal dispersivity (A_L) is estimated to be 65.5 ft. Transverse dispersivities are left unchanged, since their variability due to source scale is minimal.

f) Other Parameters

Porosity value of 0.39 was obtained from Garabedian et al., (1988) and LeBlanc et al., (1991), as part of the site characterization (Section 2.2.3).

Storativity properties such as specific yield and specific storage are not considered in the regional flow model, since these are properties related to transient simulations, and the model is simulated under the steady state assumption.

Calibration

For the calibration procedure, the main parameters consider were hydraulic conductivity, recharge, and types of boundary conditions. Anisotropy ratio, was not changed since the natural flow in the area is predominantly horizontal, and porosity was maintained constant, since this property is related only to transport phenomena.

Sensitivity analysis to recharge, boundary conditions and hydraulic conductivity were performed, as a first step. From the results of the sensitivity analyses, a single parameter was selected as a variable.

For the first simulations, the head contours reported by Savoie (1995) were used as targets to make rough adjustments to the model. Head contours are much easier to visualize than discrete points and overall trends can be quickly analyzed. However, for the most part of the calibration, discrete points were used as targets, to avoid the possible bias of the interpolation from which head contours are obtained.

The reduction of error (calculated minus observed head) was focused on the CS-4 area, analyzing results from each simulation and reviewing particularly those points clearly questionable. The thorough review of node elevations and heads for the nodes representing surface water bodies was a standard procedure for the calibration. Verification of the heads in nodes with "invoked rising water" was also a standard step after each model run, since this "invoked rising water" means that the head at those nodes has been fixed by the program as a result of the flux calculations.

The criteria for deciding complete calibration was to have a mean error less than half a foot, with all error differences of less than one foot within the CS-4 area. Results of the calibration are presented in Appendix B.

3.3.2 Pumping Schemes Simulations

Aquifer test simulation

An aquifer test in the CS-4 area was carried out by E. C. Jordan and its results are reported in the feasibility study report (E. C. Jordan, 1990). This aquifer test was simulated using the calibrated natural flow model, in order to analyze the response of the model to pumping conditions and calibrate anisotropy ratios.

To simulate this aquifer test, a new grid was constructed with more discretization and covering a smaller area of the Cape, just the area in which the actual pump test was performed. The new grid was the result of a regional-to-local interpolation, one of the resources of DYNPLOT. The simulation was run in an area of 1,540,000 ft^2. A negative (pumping) flux of 147 gpm was assigned to a node representing the pumping well used in the aquifer test.

Values of specific storage and specific yield were required by the code for transient simulations. A value of 0.35 was used for specific yield, based on the porosity value used for the steady state simulation. A value of 0.001 ft^{-1} for specific storage was considered appropriate to run the first simulation.

Head data from 7 single level monitoring wells and a multi-level well were available for the calibration of the model. The model was calibrated based on drawdown calculated in the simulation and by obtaining the measured drawdown from the log-log drawdown curves found in the feasibility study report (E. C. Jordan, 1990). The main calibration parameter was anisotropy ratio. The criteria for calibration, besides the drawdown values, were the shape of the drawdown vs. time curves and the drawdown distribution (minor to major ellipse axis ratio). Results of the calibration are presented in Appendix B.

Capture Curves Simulations

In order to fulfill the objectives of prediction of an alternative pumping scheme and analyze the flexibility of the existing one, the response of the geometry of the capture curves to different pumping scenarios was analyzed. Simulations were performed in which the objective was not the capture of the CS-4 plume. The mere analysis of resulting capture zone geometry was the goal.

To study the current well fence, the plume to capture was the CS-4 plume with the dimensions and location described by E.C. Jordan (1990). However assumptions of a bigger and/or deeper plume were made, as well.

In the process of prediction of an alternative pumping scheme, an important assumption was made. This assumption was that a well fence with fewer wells implies

less operation and maintenance costs. Another assumption determining the nature of the simulations was that the increase in pumping rate generates greater costs. For these reasons, all the simulations performed with this objective were carried out decreasing the number of wells, and maintaining the overall pumping rate.

a) Generation of Stress Conditions and Particle Starting Points

The 13 remediation wells of the existing well fence were represented in the grid as nodes. This nodes were different from the rest of the nodes of the grid because of the assignment of one dimensional elements (1-D) to them. A 1-D element is a resource of DYNFLOW, used generally for pumping nodes. A 1-D element connect the nodes of different levels so that the negative flux corresponding to pumping is equally distributed between the nodes representing the well screen.

One-dimensional elements were used in this model to connect the pumping nodes in their levels 6, 7 and 8, which elevation correspond exactly to the elevation of the screen of the remediation wells. Negative fluxes were then assigned to the desired nodes. Fluxes were assigned in cubic feet per day.

The flow model had to be run once the negative fluxes have been assigned. This simulation corresponded to a steady state, since the pumping was assumed to reach steady state in a few days, in contrast with the time of remediation, which is several years.

For the analysis of capture curves, the particle tracking was simulated under the pumping conditions. The flowfield generated in DYNFLOW with the negative fluxes representing pumping was used to run DYNTRACK. Input files to run particle tracking simulations were needed.

The simulated particles were introduced in the aquifer at certain location. Coordinates (x, y, z) were necessary for each particle. For the simulations of capture curves, two different particle tracking approaches were followed: plan view of capture zones and cross-section of the capture zone. A file with particle starting points, time of duration of the simulation and time step of data recording was constructed for both types of particle tracking simulations. This files, once generated, were used for all the different pumping schemes. The only change for each simulation was the flow field.

For the plan view output, a horizontal line of particles was used. The starting point corresponded to a location 1,500 ft upgradient of the well fence. The depth of the line of particles corresponded to the depth of the center of the plume at that location, determined from the cross-sections of the plume presented by E. C. Jordan (1990). The line had a length of 1,500 ft. In other words, the line of particles would represent a plume 700 ft wider than CS-4.

The cross-section of particles was formed by particles which starting points were also 1,500 ft upgradient of the well fence. The cross-section was formed by 286 particles, which covered an area of 183,000 ft^2 (1,500 of width and 122 ft of height). This cross-sectional area was greater then the cross-sectional area of CS-4, which is of about 31,500 ft^2. The objective was to be able to define not only if the plume was captured, but also how greater the capture zone was. The cross-section particle file was used in the "plot starting points" option of DYNPLOT, explained later in this section.

b) Particle Tracking

The particle tracking simulations were run for five years with a time step of 15 days. This means that the model followed the particles for five years, registering the location of each particle every 15 days. The particles that, after traveling the 1,500 ft distance ended at a pumping node were removed from the aquifer. This particle tracking simulations required a fairly considerable amount of computer memory, specially for the cross-section particle tracking, in which 286 particles were used. For this reason, the horizontal line simulation was always run first, and the cross-section simulation was run only in the cases in which it was considered useful.

c) Output Analysis

After each simulation, the flow field was restored in DYNPLOT and the horizontal particle tracking plotted, in plan view. After reviewing the capture curves in plan view, the need of a cross-section particle tracking simulation was decided, in each case.

Whenever more information about the capture curves geometry was needed, the cross-section simulation was run. The cross-section particle tracking was not used to plot trajectories of the particles. It was used to plot only the starting points of the particles with the DYNPLOT option "plot starting points". The plot of the starting points is only a cross-section of the aquifer showing where the particles are at the beginning of a simulation. However, a second plot was made on top of the first one, showing only the starting points of the particles that, as a result of the pumping, were removed from the aquifer.

The program compute velocities and construct individual trajectories so that it is possible to know which particles go to a pumping node, and are removed.

4. PUMPING SCHEMES ANALYSIS

The first step in the design of the groundwater treatment system is to determine the quantity of groundwater that will need to be pumped from the aquifer. The required flow rate is directly proportional to the hydraulic conductivity *K*, the hydraulic gradient *J*, and the cross-section area of the plume *A*:

$$Q = AKI$$

According to data from E.C. Jordan (1990), the cross-sectional area of the plume is 31416 ft^2. From the model results (Appendix B), the hydraulic gradient in the area is 0.0014, and the horizontal hydraulic conductivity, in the area of CS-4 plume is 191 ft/day. The discharge is then:

$$Q = (31416\ ft^2)\ (0.0014)\ (191\ ft/day) = 10,\ 500\ ft^3/day = 60\ gpm$$

The minimum overall pumping rate of any remedial system simulated needs to consider this discharge as its minimum pumping rate. As mention in the methodology, in this particular site, the existence of the operating well fence for containment, the Installation Restoration Program well fence, gave a starting point for simulations.

From the analysis of the results of each pumping scenario only in terms of the resulting heads or the horizontal particle tracking it is not possible to fully understand the geometry of the capture curves. For this reason, the cross-section of particles using the "plot starting points" option of the program (see Section 3.3.2) was the main tool in the analysis of the pumping schemes. Plotting the starting points of the particles that are removed from the aquifer due to pumping a cross-section of the capture zone is obtained. This cross-section of the capture zone is perpendicular to the groundwater flow and is located 1,500 ft upgradient of the well fence. In each one of the figures of cross-section of

particles presented in the next sections, the larger dots represent the cross-section of the capture zone, 1,500 feet upgradient of the well fence. As shown in Figure 4.1, the CS-4 plume falls within the cross-sectional area defined by the particles.

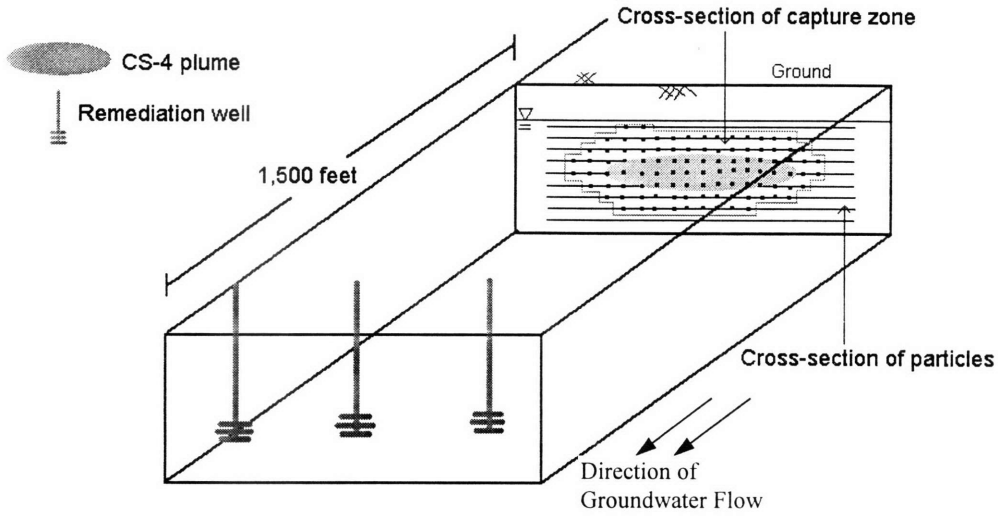

Figure 4.1. Diagram explaining the meaning of the "plot starting points" figures, used to analyze the geometry of the capture curves resulting from the different pumping schemes (Figure shows only three wells for simplicity).

4.1 Analysis of the Capture Zones Under Different Pumping Schemes

To evaluate the effects of well spacing and pumping rates in the geometry of the capture zone, six simulations were run. The first 4 simulations, corresponding to the analysis of the increase in overall pumping rate to compensate well spacing, were run with just three wells. In Table 4.1 the pumping schemes for this simulations are shown.

Table 4.1. Simulations to analyze the response of the capture curve geometry to different pumping rates and well spacing, for a three-well fence. A small theoretical plume (not CS-4 plume) is used for this analysis.

Simulation	Wells operating	Pumping rate (gpm)	Individual pumping rate (gpm)	Distance between wells (ft)
1	9, 7, 5	90	30, 30, 30	120
2	10, 7, 4	90	30, 30, 30	180
3	10, 7, 4	135	45, 45, 45	180
4	10, 7, 4	165	55, 55, 55	180
5	11, 7, 3	210	70, 70, 70	240

For the first simulation, a capture zone of about 39,000 ft^2 in cross-sectional area with a width of less than 600 ft was obtained. This pumping scheme was the basis for the changes in pumping and well spacing of the next four simulations.

Moving the wells so that they were 180 ft apart, without increasing the pumping rate gave a clearly inefficient pumping scheme, in which particles escape the well fence passing between the pumping wells. This was observed in the plan view of the capture zone (Figure 4.2).

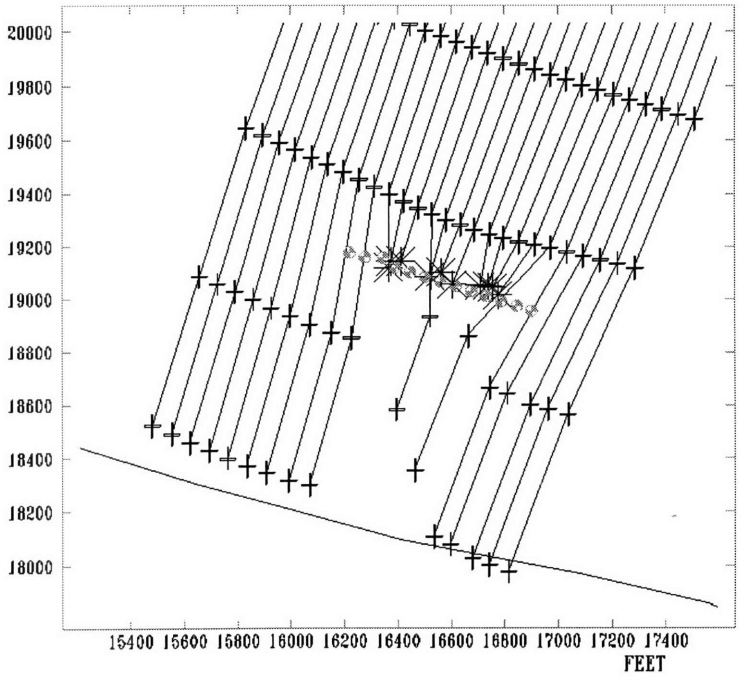

Figure 4.2. Particles escaping a three-well fence due to an inappropriate well spacing of 180 feet, for a total pumping rate of 90 gpm (simulation 2 in Table 4.1.)

The third simulation was run increasing the pumping rate by 50%. In this case, the analysis of the horizontal particle tracking indicated that no particles in the center of the theoretical plume would escape the capture zone. Based on these results, a cross-section of particles was analyzed. In Figure 4.3 it can be observed that the cross-sectional capture zone did not have the elliptical form convenient for the proper removal of contaminants.

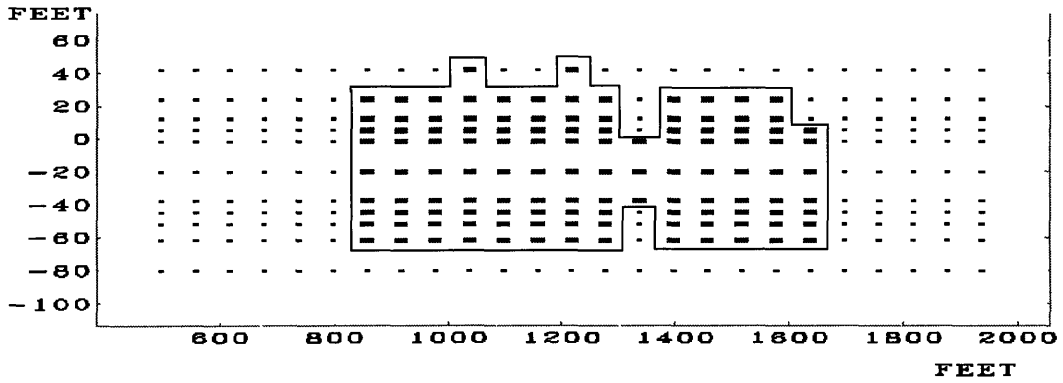

Figure 4.3. Cross-section of the capture zone for 3 wells, 180 feet apart, pumping 45 gpm individually.

The particles which reach the well fence in the middle of pumping wells may or may not be captured, depending on the distribution of hydraulic control. In this simulation, particles between the wells 4 and 7 were not captured. They reached the well fence at the midpoint between wells, where zones of greater head value are formed, as seen in Figure 4.4.

In the fourth simulation, however, increasing the pumping rate about 80% of the original rate (going from 90 gpm to 210 gpm), it was finally possible to completely extend the hydraulic control, defining an elliptical capture zone (Figure 4.5). A great difference in cross-sectional area of the capture zone was obtained from simulations 1 and 4 (see Table 4.1). This was the result of an increase in well fence length and an increase in pumping rate. The new cross-sectional area was approximately 75,000 ft^2, which is about twice as bigger as the first capture zone. This is easily explained because an increase in the well fence length, as well as an increase in pumping rate were done.

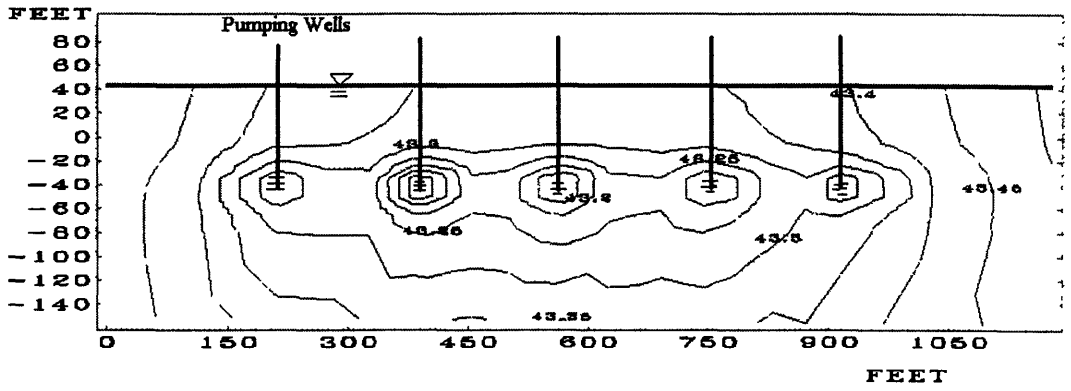

Figure 4.4. Head distribution around pumping wells. Head is lower near the wells and areas of greater values of head are located in the midpoint between wells. Example of five-well system.

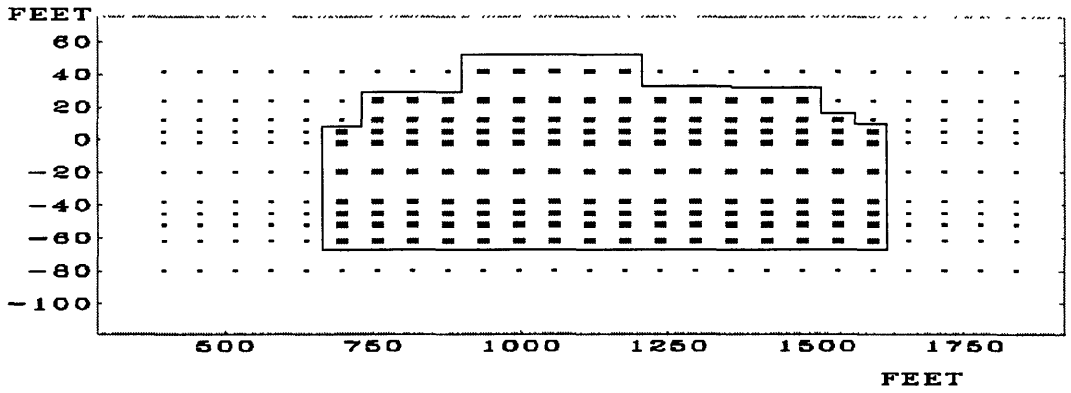

Figure 4.5. Cross-section of the capture curve generated by pumping 165 gpm with 3 wells (see Table 4.1). The larger dots represent the capture zone cross-sectional area.

Well spacing is one of the decision variables for a remedial or containment system. As mentioned in Section 3.1, different approaches have been used to define proper well locations. Use of simulation and optimization to control hydraulic gradients (Gorelick et al., 1993), constraining groundwater velocities (Heidari et al., 1987), and use of three-dimensional simulations combined with mixed-integer programming (Sawyer et al., 1995) are some of the examples given.

Analytical solutions have also been developed (Javandel and Tsang, 1987; Yang et al., 1995). Javandel and Tsang (1987) explain that in general, when the distance

between two wells is too large for a given discharge rate, a stagnation point will be formed behind each pumping well, and some particles are able to escape from the interval between the two wells. When the distance between the two wells is reduced while keeping the discharge rate constant, eventually a position will be reached where only one stagnation point will appear. In this case, no particles can escape from the space between the two wells. Similarly, increasing the discharge rate, as shown in the previous results, can compensate the well spacing, up to a certain point. These authors develop analytical solutions useful to calculate well spacing. However, the solutions are based on fully penetrating wells in homogeneous and isotropic aquifers of uniform thickness.

The advantage of a the three-dimensional numerical model, as the one used in this study, is that the location of wells can be planned according to the results of simulations and much more complex scenarios can be modeled and evaluated.

An interesting result came from the simulation of three wells, 240 ft apart, pumping at 70 gpm each. In Figure 4.6, a plan view showing particle tracking and head contours is presented. It can be seen that one of the particles simulated escaped the well fence . This particle passed between the wells 7 and 3. However, in the other side of the well fence all particles were captured.

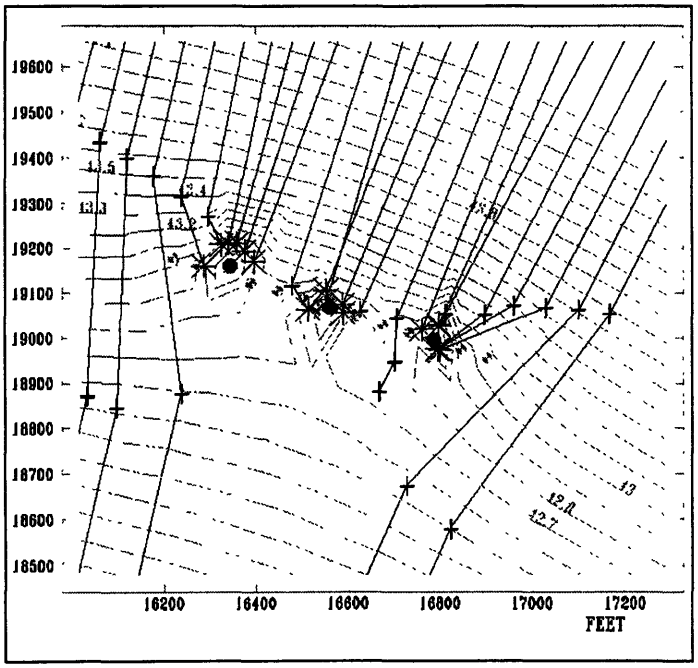

Figure 4.6. Capture curve resulting from a three-well option (simulation 5 in Table 4.1). The head distribution and the hydraulic control are asymmetric result of the well fence asymmetry.

As described in Section 2.3.3, the well number 11 of the well fence, is not aligned as the rest of the wells. This can be the reason for the asymmetry of the capture curve, in terms of drawdown and stagnation points distribution. The stagnation points generated while pumping to remediate a site are important parameters of hydraulic control and can cause inefficient performance of the system. Stagnation points may cause particles to escape (Javandel and Tsang, 1987), and can also be the reason of increasing the time for cleanup, since it is in this stagnation points where the water does not move or move really slowly (Hoffman, 1993). In general, different well location will cause a different location of the stagnation points and then a different performance of the remedial system.

In this case, a single simulation is not enough to conclude that the different location of the well number 11 is beneficial in terms of capturing the contaminants for the given pumping scheme. Irregularities in the model discretization may also affect this result. In Figure 4.6, the head contours shown are not smooth and are formed by straight lines. This is the result of the interpolation from the elements forming the grid. Discretization might slightly affect results. However, it is interesting to review this simulation and mention the fact that well location is a very important parameter to consider while designing a remedial or containment system. Locating the wells not necessarily in a straight line may result in different hydraulic control.

All previous results come from equally-spaced wells. Different ways to achieve hydraulic control were also evaluated having non-equally-spaced wells.

The results from the simulation of six non-equally-spaced wells indicate that this option is less effective than the equally-spaced option. However, a solid capture curve could be achieved with a proper combination of pumping rates (Figure 4.7). Pumping rates are presented in Table 4.2 for two different simulations. For the first one, with an overall discharge of 220 gpm, some of the particles escaped the well fence. In the second case, increasing the pumping and redistributing it, the capture zone was attained.

Table 4.2. Simulations to analyze the response of the capture curve geometry to different pumping rates with non-uniform well spacing. A small theoretical plume (not CS-4 plume) is used for this analysis.

Simulation	Wells operating	Pumping rate (gpm)	Individual pumping rate (gpm)	Distance between wells (ft)
1	13, 10, 8, 6, 4, 1	220	50, 30, 30, 30, 30, 50	180, 120, 120, 120, 180
2	13, 10, 8, 6, 4, 1	240	50, 40, 30, 30, 40, 50	180, 120, 120, 120, 180

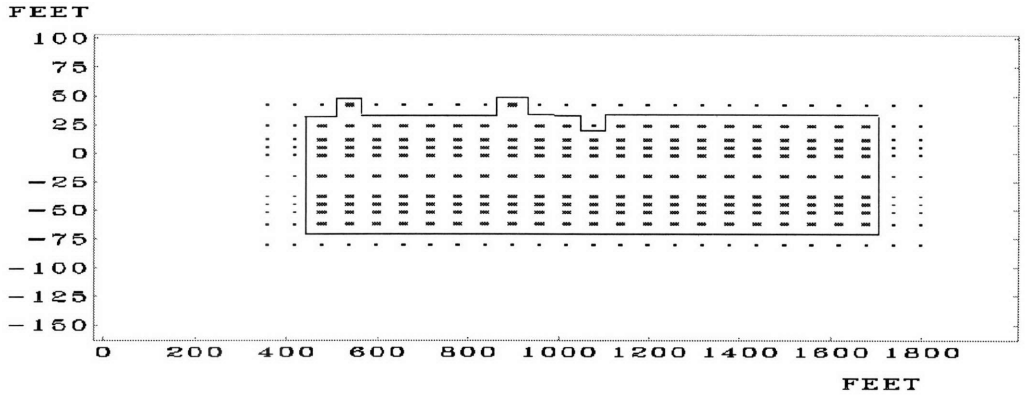

Figure 4.7. Cross-section of the capture curve generated by six wells, pumping 240 gpm, as indicated in Table 4.2 (simulation number 2).

4.2 Flexibility of the Current Well Fence

The Installation Restoration Program well fence was simulated. A particle tracking simulation using 13 wells pumping 140 gpm, located 60 ft apart as in the IRP well fence, was run (see Section 2.3.3). According to Figure 4.8, the pumping rate and the number and spacing of wells can be considered adequate. In this horizontal view, a capture curve approximately 1100 ft wide is observed. From the analysis of the cross-section of particles and the "plot starting points" output, the vertical and horizontal effects of the pumping scheme can be considered sufficient for the capture of the plume (Figure 4.9). The capture zone is approximately 250 ft wider and 25 ft thicker than CS-4. The area of the ellipse formed by the plume was of 31,400 ft^2. The area of the ellipse formed

by the capture zone was about 64,800 ft^2. The cross-section of the capture zone is then two times bigger than the cross-section area of the plume. This guarantee the removal of all contaminated water.

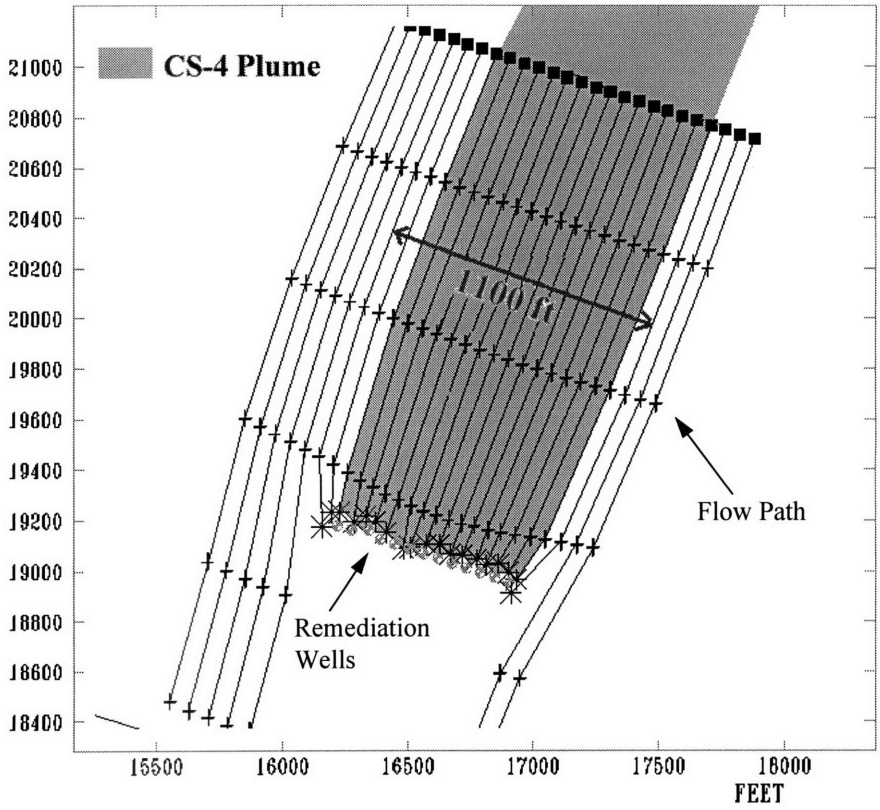

Figure 4.8. Two-dimensional horizontal capture curve resulting from the simulation of the existing pumping scheme at MMR.

To analyze what could be done with the existing containment system, in response to a bigger or deeper plume, simulations using the current well fence but increasing the pumping rate were made and the extent of the resulting capture zones analyzed. Results are presented in Table 4.3.

Table 4.3. Enlargement of the capture curve using 13 wells, in response to the increase of pumping rates, distributing the stress equally throughout the well fence.

Pumping Rate (gpm)	Wide (ft)	Thickness (ft)	Cross-sectional Area (ft^2)	% increase in cross-sectional area	Elevation of lower limit (ft msl)
140*	1100	75	64, 800	-	-65
182	1100	85	73, 400	13	-65
200	1100	85	73, 400	13	-65
220	1220	85	81, 400	26	-65
250	1220	105	100, 600	55	-65

* IRP well fence

Results shown in this table indicate that the increase in the vertical extent of the capture zone was apparently due to water coming from the upper side (i.e., the water table side) of the capture zone. No change in the lower limit of the capture zone was registered in any of the simulations run, while the upper limit significantly changed.

A factor that can contribute to this response is the lower conductivity of the deepest layer of the aquifer. This layer has a conductivity of 35 ft/day, whereas the layer in the middle and the upper-most layer have values of 120 ft/day and 217 ft/day respectively. Another very important factor contributing to this effect is the anisotropy ratio, which is about three times bigger in the lower part of the aquifer (see Figure 3.3). It is easier for the water to flow to the well from the upper layer. It is also important to have in mind the degree of resolution of the cross-section used for particle tracking. The lower-most line of particles is located 20 ft below the lower line of particles captured. Any increase in the thickness of the capture zone of less than 20 ft in the bottom part of the aquifer could not be detected because there were no particles in that area that could indicate the enlargement of the capture curves. Nevertheless, it was clear that the increase in thickness was in general due to the capture of more water from the water table side.

In the horizontal, the capture zone increased in less proportion than it did in the vertical. With an increase of 110 gpm (from 140 to 250 gpm), the capture zone increased approximately 30 ft in the vertical, corresponding to more than 3 ft per unit of pumping (gpm). In the horizontal, the capture zone increased about 120 ft, which corresponded to

less than 1 ft per unit of pumping. These proportions, however, are mentioned merely to illustrate the main results, and can not be considered as design parameters.

According to the results presented in Table 4.3, pumping 220 gpm, the well fence will capture a plume about 50% bigger than CS-4 plume. However, if the plume is located deeper in the aquifer, the sole increase in pumping rate will not be effective, since the lower limit of the capture zone do not go deeper even for a pump rate 75% larger than the original pump rate of 140 gpm. Placing the well screens deeper into the aquifer could be a more effective way to contain a deeper plume, than increasing the pumping rate. Faybishenko, et al. (1995) analyze the hydrodynamics of the capture zone of a partially penetrating well, and conclude, as one would expect, that the maximum vertical extent of the capture surface increases as the degree of penetration increases. Although this analysis is for a confined aquifer, very similar results are expected in the Cape Cod aquifer, since the amount of drawdown relative to the total saturated thickness of the aquifer is very small.

After the analysis of the different ways in which the pumping scheme currently in operation can be modified to respond to a different plume, an analysis of the response to technical problems related to the well fence itself was performed.

The assumption of one of the wells out of operation was made. The simulations to determine the different pumping strategies necessaries to achieve a similar capture curve were performed, changing the location of the non-operating well. The results indicate that such a situation can be easily solved by increasing the pumping rate of the wells adjacent to the well out of operation. The capture curves obtained from the normal situation and the 12-well operation are very similar (Figure 4.9 a and b).

Figure 4.9 shows how the capture zones of both pumping schemes were effective, and in fact, were practically the same. In the case of the 12-well situation, the well number 10 have been turned off, and wells 11 and 9 are pumping 15 gpm, instead of 10 gpm, which is the rate of pumping in the normal situation. The increase in pumping rate easily offset the negative effect (i.e., loss in hydraulic control) of a non-operating well.

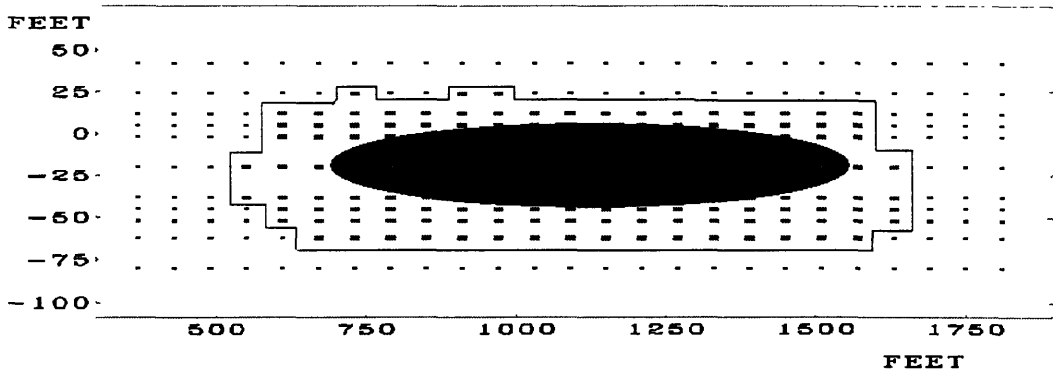

a

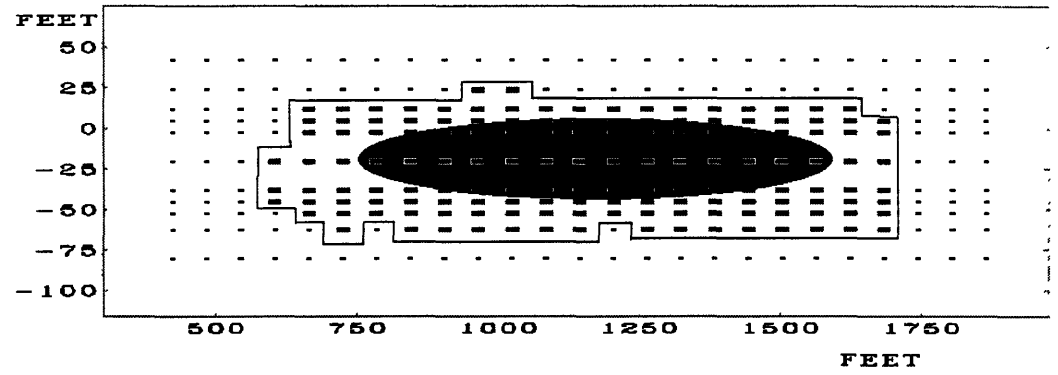

b

Figure 4.9. Comparison of capture curves obtained from the current pumping scheme (a), and the well fence with one of the wells out of operation with a different pumping rate distribution, but maintaining the overall pumping rate of 140 gpm (b).

4.3 Prediction of an Alternative Pumping Scheme

After the analysis of the current well fence of 13 wells, and the response of the aquifer to different pumping scenarios, the option of an alternative containment system was addressed. The different simulations run for this purpose are presented in Table 4.4.

Table 4.4. Simulations to predict an alternative effective capture zone for CS-4 plume. Simulations were run according to the dimensions of the plume reported by E. C. Jordan (1990).

Number of wells	Wells operating	Pumping rate (gpm)	Individual pumping rate (gpm)	Distance between wells (ft)
8	13, 11, 10, 8, 7, 5, 3, 1	140	20 in the outside wells and 16.7 at the rest of the wells	102
8	13, 11, 10, 8, 7, 5, 3, 1	140	17.5	102
7	13, 11, 9, 7, 5, 3, 1	140	20	120
5	13, 10, 7, 4, 1	140	28	180

All simulations were run with schemes of equally-spaced wells, based in the results of the six well simulation, described above. In the six-well simulation was clear that an option of non-equally spaced wells presents disadvantages with respect to the uniformly-spaced options. Although a combination of pumping rates can be found that satisfies the requirements for capturing the plume, these pumping rates may be too high with respect to the ones from equally-spaced options.

As indicated in the Table 4.4, the first simulation of eight wells was run with a non-uniform pumping, based on the fact that the IRP well fence works with more pumping in the wells located at the sides (see Section 2.3.3). However, the second simulation was run pumping equally from each well. The results in the cross-section capture zone were very similar in terms of the shape of the capture zone and almost identical in terms of cross-sectional area, which was about 64,800 ft^2.

Since fewer wells for a fixed pumping rate (140 gpm) presumably implies reduction in the operation and maintenance costs, a simulation of seven wells was performed.

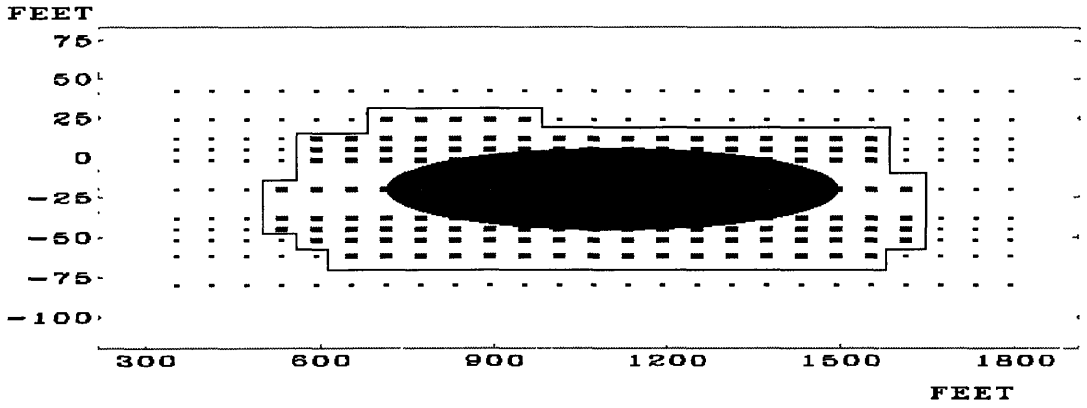

Figure 4.10. Cross-section of the capture curve resulting from seven-well option, in which the overall pumping rate is 140 gpm

The area of the seven-well pumping strategy was approximately 64,800 ft^2, as in the eight well simulations (Figure 4.10). Interestingly, the existing pumping scheme of 13 wells resulted in a very similar cross-sectional area.

The seven-well option is preferred over the eight-well option because both produced the same results, and in the eight-well system the wells had to be relocated. This relocation of wells would imply costs, not needed for the seven-well option.

The next simulation was done with five wells using 140 gpm overall discharge. As expected, that pumping rate was not enough to capture the CS-4 plume, since well spacing becomes fairly important. The objective then, was to increase the pumping rate until the proper capture zone were achieved.

An increase of more than 40% was necessary to obtain a horizontal capture curve output without particles passing between wells. A cross-sectional particle tracking was run and it was observed that this pumping rate resulted in a capture zone of approximately 79,000 ft^2, which was greater than the one obtained from 13, 8 and 7 wells. The greater capture zone from the five well simulation implies the capture of a larger proportion of clean water, which makes this option less effective. This, however, was not the only disadvantage of the five-well option, since when the cross-section was analyzed, it could be seen that the cross-section of the capture zone did not show the uniform ellipsoidal shape observed for seven, eight or 13 wells (Figures 4.9 and 4.10).

The cross-sectional shape of the capture zone was very similar to the one obtained for three wells pumping a total rate 135 gpm, shown in Figure 4.3 as an example of inefficient pumping scheme.

It is important to mention, as a first consideration, that all calculations of area and observations of cross-sectional shape of the capture zones, are based on the particle tracking of 286 particles (procedure described in Section 3.3). The degree of resolution limits the exact definition of the cross-sectional shape. It is of course likely that the three different pumping schemes considered effective (7, 8 and 13 wells) derive in different cross-section area of the capture zones. However, from the results of this study, no significant changes were observed, which lead to the proposal of an alternative system.

The explanation for the fact that 13, and 7 wells gave as a result practically the same capture curve geometry, must be based on the well spacing to pumping rate relationship. The seven-well alternative consisted of wells located at 120 ft apart, which is twice the distance of the wells in the current well fence. The pumping rate for each individual well was increased, although the overall pumping rate was maintained constant. The results showed that the negative effect of increasing distance between wells was offset by the positive effect of increasing individual pumping rates.

After analyzing the results from these candidate alternative pumping scenarios, the seven well option seems to be a good alternative pumping scheme. The operation and maintenance cost would be reduced and the capture of CS-4 plume would still be attained. However, other factors, technical and non-technical have to be considered to make decision about changing the existing pumping scheme.

Aquifer heterogeneity is a factor that may influence the geometry of capture zones for a given pumping condition. As mentioned in Section 4.2, differences in hydraulic conductivity lead to different amounts of water drawn from distinct lithologic units. The effect discussed in Section 4.2 is due to the existence of a low conductivity layer at the bottom of the aquifer. However, heterogeneity may also exist within layers, and this is not represented in the model. For this model the layers are assumed to be homogeneous (see Figure 3.3), and effects of changes in hydraulic conductivity due to the presence of lenses of different materials, can not be observed in the results of this study.

Heterogeneity is present in the Mashpee Pitted Plain, as indicated by Foster-Reid (1994) and Springer (1991). The large-scale heterogeneity, characterized by Springer (1991), as well as small scale heterogeneity may have effects on the geometry of the capture zones, once a well fence is operating. It is recommended that numerical simulations similar to those used in this study be developed to evaluate the sensitivity of the capture zone to heterogeneity.

As mentioned in Section 3.1, the opportunity to evaluate a large number of alternatives combining different factors is one of the greatest advantages of the use of a three-dimensional numerical model to help in the design of remedial or containment systems. The natural flow model developed in this study can be used to evaluate a great number of capture zone options. This can be done not only to design or evaluate a containment system, which was the objective of this study, but also to design a remediation scheme, by moving some of the wells to the points of maximum concentration of contaminants.

5. CONCLUSIONS

The first objective of this study was to develop a groundwater flow model to get a comprehensive understanding of the groundwater system at Cape Cod. Using the model as a tool, different pumping schemes for the extraction of contaminated groundwater were analyzed. The final purpose of this work was to study different characteristics of the containment pumping system existing at the site, and to predict an alternative pumping scheme.

From the findings of this study, the following conclusions can be made:

Well fences of seven and eight equally-spaced wells, pumping a total of 140 gpm uniformly distributed, resulted in very similar capture zone geometry. These geometry are also very similar to the capture curve resulting from the pumping scheme currently operating at the MMR.

Since the seven well simulations corresponded to wells that are part of the existing well fence, this seven well system would be an effective alternative pumping scheme for the containment of CS-4. The operation and maintenance costs would presumably be reduced and the capture of the plume would still be attained.

The 13-well pumping scheme currently operating at the MMR showed interesting features regarding the different ways in which can be operated to respond to different field conditions. The 13-well system showed great flexibility in terms of achieving the same capture curves geometry when one of the wells can not be operated. The increase in pumping rate in the adjacent wells clearly offsets the loss in hydraulic control due to the missing well.

Supporting the conclusion stated above, the seven-well system proposed as an alternative proves that the redistribution of pumping rates is very effective to generate adequate capture zones. However, other results showed that as well spacing increases considerably, the increase in pumping rates may not be the best option to achieve an effective capture zone. In such cases, relocation of wells should be considered.

If as a result of monitoring and an improved site characterization, the CS-4 plume were redefined as a bigger or deeper plume, the existing well fence could be modified in its operation and still capture the contaminants. Increasing pumping rates with the 13-well, results in an increase of the capture curve dimensions.

An increase in pumping rate resulted in an expansion of the height of the capture zone. The amount of water drawn from the lower portion of the aquifer remained approximately constant, and thus the effect of this increase in pumping rate is more noticeable in the upper section of the aquifer. This might be result of the lower conductivities (horizontal and vertical) of the lower part of the aquifer. Therefore, to capture a deeper plume, the increase in pumping rates may not be the most effective alternative. A better option would be to place the wells deeper in the aquifer.

Aquifer heterogeneity is a factor that may influence the geometry of capture zones for a given pumping condition. Simulations to explore the influence of heterogeneity are recommended.

As a general conclusion, to provide the necessary hydraulic control for the containment of the CS-4 plume, the 13-well fence currently operating at the MMR proved to be effective and flexible. Modifications to this pumping scheme will need to consider well spacing, well screen depth and pumping rate distribution.

6. References

ABB Environmental Services Inc. 1992a. *Groundwater Focused Feasibility Study, West Truck Road Motor Pool (AOC CS-4)*, Installation Restoration Program, Massachusetts Military Reservation, prepared for HAZWRAP, Portland ME, February 1992.

ABB Environmental Services Inc. 1992b. *Record of Decision Interim Remedial Action West Truck Road Motor Pool (AOC CS-4) Groundwater Operable Unit*, Installation Restoration Program, Massachusetts Military Reservation, prepared for HAZWRAP; Portland ME, May 1992.

ABB Environmental Services Inc. 1992c. *CS-4 Groundwater Operable Unit. Extraction and Treatment System. Final Design Package, Volume I, Drawings and Technical Specifications*, Installation Restoration Program, Massachusetts Military Reservation, prepared for HAZWRAP, Portland ME, July 1992.

ABB Environmental Services Inc. 1996. *Personal communication*, March, 1996

Ahlfeld, D. P., and Sawyer, C. S. 1990. Well Location in Capture Zone Design Using Simulation and Optimization Techniques, *Ground Water*, 28(4), 507-512.

Bair, E.S. and C. Road 1992. *Comparison of Flow Models Used to Delineate Capture Zones of Wells: 1. Leaky-Confined Fractured-Carbonate Aquifer.* Ground Water. 30(2). 199-211.

Barlow, P.M. and Hess K.M. 1993. *Simulated Hydrologic Responses of the Quashnet River Stream-Aquifer System to Proposed Ground Water Withdrawals*; U.S. Geological Survey Water-Resources Investigation Report 93-4064, 52p.

Bartow, G., and Davenport, C. 1995. Pump-and-Treat Accomplishments: A Review of the Effectiveness of Ground Water Remediation in Santa Clara Valley, California, *GWMR*, Spring, 140-146.

Camp Dresser McKee, Inc. 1992. *Dynsystem, Groundwater flow and transport modeling system*, Reference Guide.

Cape Cod Commission. 1996. *CapeTrends, Demographic and Economic Characteristics and Trends; Barnstable County- Cape Cod*, 3rd. Ed., Barnstable MA.

E.C. Jordan Co. 1989a. *Site Inspection Report, Field Investigation Report Conducted Fall 1987, Task 2-3A*, Installation Restoration Program, Massachusetts Military Reservation, prepared for HAZWRAP, Portland ME, March 1989.

E.C. Jordan Co. 1989b. *Hydrogeologic Summary Report, Task 1-8*, Installation Restoration Program, Massachusetts Military Reservation, prepared for HAZWRAP, Portland ME, April 1989b.

E.C. Jordan Co. 1989c. *Site Inspection Report, Field Investigation Work Conducted Spring-Summer 1988, Task 2-3B,* Installation Restoration Program, Massachusetts Military Reservation, prepared for HAZWRAP, Portland ME, July 1989.

E.C. Jordan Co. 1990. *Groundwater Feasibility Study, Study Area CS-4*, Installation Restoration Program, Massachusetts Military Reservation, prepared for HAZWRAP, Portland ME; October 1990.

Faybishenko, B.A., I. Javandel, P.A. Witherspoon. 1995. *Hydrodynamics of the Capture Zone of a Partially Penetrating Well in a Confined Aquifer.* Water Resources Research. 31(4). 859-866.

Foster-Reid, G. H., 1994. *Variability of Hydraulic Conductivity and Sorption in a Heterogeneous Aquifer*, M.S. Thesis, Department of Civil and Environmental Engineering, Massachusetts Institute of Technology, Cambridge.

Freeze, R.A. and J.A. Cherry. 1979. *Groundwater*. Prentice Hall. New Jersey.

Gailey, R.M. and S.M. Gorelick. 1993. *Design of Optimal Reliable Capture Schemes: Application to the Gloucester Landfill Ground-Water Contamination Problem.* Ground Water. 31(1). 107-114.

Garabedian, S. P., Gelhar, L. W., and Celia, M. A. 1988. *Large-Scale Dispersive Transport in Aquifers: Field Experiments and Reactive Transport Theory*, Report 315, Ralph M. Parsons Laboratory, Department of Civil and Environmental Engineering, Massachusetts Institute of Technology, Cambridge MA.

Garabedian, S. P., LeBlanc, D. R., Gelhar, L. W., and Celia, M. A. 1991. Large-Scale Natural Gradient Tracer Test in Sand and Gravel, Cape Cod, Massachusetts. Section 2: Analysis of Spatial Moments for a Nonreactive Tracer, *Water Resources Research*, 27(5), 911-924.

Gelhar, L. W., Welty, C., and Rehfeldt, K. R. 1992. A Critical Review of Data on Field-Scale Dispersion in Aquifers, *Water Resources Research*, 28(7), 1955-1974.

Gelhar, L. W., 1996 .*Personal communication*, April 1996.

Gillham, R. W. 1995. *In Situ Treatment of Groundwater: Metal-Enhanced Degradation of Chlorinated Organic Contaminants*, Recent Advances in Ground-Water Pollution Control and Remediation, A NATO Advanced Study, Institute Kemer, Antalya, Turkey, May 20 - June 1, Springer-Verlag, New York.

Gorelick, S.M., R.A. Freeze, D. Donohue, J.F. Keely. 1993. Groundwater Contamination-Optimal Capture and Containment. Lewis Publishers. Boca Raton. FL. 385 pp.

Guswa, J. H., and LeBlanc, D. R. 1985. *Digital Models of Groundwater Flow in the Cape Cod Aquifer System, Massachusetts*, U.S. Geological Survey, Water Supply Paper.

Hayes, M. F. Jr. 1996. *Stimulating In Situ groundwater Bioremediation via Sparging: Gas Flow, Groundwater Flow, and Mass Transfer in the Biosparge Zone*, M.S Thesis, Department of Civil and Environmental Engineering, Massachusetts Institute of Technology.

Heidari, M., J. Sadeghipour, O. Drici. 1987. *Velocity Control as a Tool for Optimal Plume Containment in the Equus beds Aquifer, Kansas*. Water Resources Bulletin. 23(2). 325-355.

Hoffman, F. 1993.Smart Pump and Treat, *Ground Water*, 31(1), 98-102.

Isherwood, W., Rice, D. Jr., Ziagos, J. and Nichols, E. 1993. Smart Pump and Treat, *Journal of Hazardous Materials*, 35 (1993), 413-426.

Javandel, I. and C. Tsang. 1986. *Capture-Zone Type Curves: A tool for Aquifer Cleanup.* Ground Water. 24(5). 616-625.

Khachikian, C. S. 1996. *Sorption of Chlorinated Solvents in a Sandy Aquifer*, Master of Engineering Thesis, Department of Civil and Environmental Engineering, Massachusetts Institute of Technology, Cambridge.

Lázaro, A. M. 1996. *Simulation of Groundwater Contaminant Plume in a Sand and Gravel Aquifer in Cape Cod, Massachusetts Using a 3D Model*, Master of Engineering Thesis, Department of Civil and Environmental Engineering, Massachusetts Institute of Technology, Cambridge.

LeBlanc, D. R. 1984. *Digital Modeling of Solute Transport in a Plume of Sewage-Contaminated Ground Water, Movement and Fate of Solutes in a Plume of Sewage-Contaminated Ground Water, Cape Cod, Massachusetts*, U.S. Geological Survey Toxic Waste Ground-Water Contamination Program, U.S. Geological Survey Open File Report, 84-475, 11-45.

LeBlanc, D. R., Guswa, J. H., Frimpter, M. H., and Londquist, C. J. 1986. *Ground-Water Resources of Cape Cod, Massachusetts*, Hydrological Investigation Atlas, HA-692, 4 sheets, U.S. Geological Survey, Reston, Va.

LeBlanc, D. R., Garabedian, S. P., Hess, K. M., Gelhar, L. W., Quadri, R. D., Stollenwerk, K. G., and Wood, W. W. 1991. Large-Scale Natural Gradient Tracer Test in Sand and Gravel, Cape Cod, Massachusetts. Section 1: Experimental Design and Observed Tracer Movement, *Water Resources Research*, 27(5), 895-910.

MacDonald, J. A. and Kavanaugh, M. C. 1994. Restoring Contaminated Groundwater: An Achievable Goal? *Environmental Science and Technology*, 28(8), 362-368.

Mackay, D. M. and Cherry, J. A. 1989. Groundwater Contamination: Pump-and Treat Remediation, *Environmental Science and Technology*, 23(6), 630-636.

Massachusetts Executive Office of Environmental Affairs. 1994. *Water Resources of Cape Cod: Water Use, Hydrology, and Potential Changes in Ground Water Levels*, Department of Environmental Management, Office of Water Resources, October 1994.

Masterson, J.P. and P.M. Barlow, 1994. *Effects of Simulated Ground-water Pumping and Recharge on Ground-Water Flow in Cape Code, Martha's Vineyard, and Nantucket Island Basins, Massachusetts.* US Geological Survey. Open-File Report 94-316.

Mercer, J. W. and Skipp, D. 1990. Considerations in the Design of Pump and Treat Remediation Systems. *Superfund '90. Proceedings of the 11th National Conference.* Hazardous Materials Control Research Institute.

Nyer, E. K. 1994. Where is the Money? *Groundwater Monitoring Review.* Spring 1994. 100-104.

Oldale, R.N. 1969.Seismics Investigations in Cape Cod, Martha's Vineyard, and Nantucket, Massachusetts, and a Topographic Map of the Basement Surface from Cape Cod Bay to the Islands; *Geological Survey Research*; U.S. Geological Survey Professional Paper 650-B; pp. B122-B127.

Oldale, R. N. 1982. Pleistocene Stratigraphy of Nantucket, Martha's Vineyard, the Elizabeth Islands, and Cape Cod, Massachusetts, in *Wisconsian Glaciation of New England*, edited by G. J. Larson and B. D. Stone, pp. 1-34, Kendall/Hunt, Dubuque, Iowa.

Oldale, R. N., and Barlow, R. A. 1987. Geologic Map of Cape Cod and the Island, Massachusetts, *Misc. Invest. Ser., Map I-1763*, U.S. Geological Survey, Reston, VA..

Parmentier, P. P., and R. M. Klemovich. 1996. A New Direction in Remediation. *Civil Engineering*, April.

Picazo, C. L., 1996. *Human Health Risk Assessment of Chemical Spill 4 at the Massachusetts Military Reservation.* Master of Engineering thesis, Massachusetts Institute of Technology. Cambridge.

Rajaram, H. and Gelhar, L.W. 1995. Plume-Scale Dependent Dispersion in Aquifers with a Wide Range of Scales of Heterogeneity, *Water Resources Research*, 31(10), 2469-2482.

Savoie, J. 1993. *Altitude and Configuration of the Water Table, Western Cape Cod, Massachusetts*. US Geological Survey Open-File Report 94-462.

Sawyer, C.S., Ahlfeld, D.P., A.J. King. 1995. *Groundwater Remediation Design Using a Three-Dimensional Simulation Model and Mixed-Integer Programming.* Water Resources Research. 31(5). 1373-1385.

Schwarzenbach, R. P. And J. Westall. 1981.Transport of Nonpolar Organic Compounds from Surface Water to Groundwater. Laboratory Sorption Studies, *Environmental Science and Technology*, 15, 1360-1367.

Schwarzenbach, R. P., P.M. Gschwend, D.M. Imboden. 1993. *Environmental Organic Chemistry*, Wiley, New York, NY.

Semprini, L.; Hopkins, G. D.; Roberts, P. V.; McCarty, P. L. 1990. A Field Evaluation of In Situ Biodegradation of Chlorinated Ethenes: Part 2, Results of Biostimulation and Biotransformation Experiments. *Ground Water*, Vol. 28, No. 5, pp. 715-727.

Semprini, L., Hopkins, G. D.; Roberts, P. V.; McCarty, P. L. 1991a. A Field Evaluation of In Situ Biodegradation of Chlorinated Ethenes: Part 3, Studies of competitive Inhibition. *Ground Water*, Vol. 29, No. 2, pp. 239-250.

Semprini, L.; McCarty, P. L. 1991b. Comparison Between Model Simulations and Field Results for In Situ Biorestoration of Chlorinated Aliphatics: Part 1. Biostimulation of Methanotrophic Bacteria. *Ground Water*, Vol. 29, No. 3, pp. 365-374.

Semprini, L.; McCarty, P. L. 1992a. Comparison Between Model Simulations and Field Results for In Situ Biorestoration of Chlorinated Aliphatics: Part 2. Cometabolic Transformations. *Ground Water*, Vol. 30, No.1, pp. 37-44.

Semprini, L.; Hopkins, G. D.; Roberts, P. V.; McCarty, P. L. 1992b. Pilot Scale Field Studies of In Situ Bioremediation of Chlorinated Solvents. *Journal of Hazardous Materials*, Vol. 32, pp. 145-162.

Skiadas, P. 1996. *Design of an In Situ Bioremediation Scheme of Chlorinated Solvents Sequenced by Cometabolic Oxidation.* Master of Engineering Thesis. Massachusetts Institute of Technology. Cambridge, MA.

Springer, A.E. and E.S. Bair. 1992. *Comparison of Methods Used to Delineate Capture Zones of Wells: Stratified-Drift Buried-VAlley Aquifer.* Ground Water. 30(6). 908-917.

Springer, R.H. 1991. *Application of an Improved Slug Test Analysis to the Large-Scale Characterization of the Heterogeneity in a Cape Cod Aquifer.* Master of Science Thesis. Massachusetts Institute of Technology. Cambridge, Massachusetts.

Stenzel, M. H., Merz, W. J., 1989. Use of Carbon Adsorption Processes in groundwater treatment. *Environmental Progress*, 8(4).

Thompson, K. D., 1994. *The Stochastic Characterization of Glacial Aquifers Using Geologic Information,* Ph.D. Thesis, Department of Civil and Environmental Engineering, Massachusetts Institute of Technology, Cambridge.

Tillman, D. E., 1996. *Combination of Zero-valent Iron and Granular Activated Carbon for the Treatment of Groundwater Contaminated With Chlorinated Solvents*, Master of Engineering Thesis, Department of Civil and Environmental Engineering, Massachusetts Institute of Technology, Cambridge.

Travis, C. C. and Doty, C. B. 1990. Can Contaminated Aquifers at Superfund Sites be Remediated? *Environmental Science and Technology*, 24(10), 1464-1466.

van der Kamp, G.; Luba, L. D.; Cherry, J. A.; and Maathuis, H. Field Study of a Long and Very Narrow Contaminant Plume; *Ground Water*, Vol. 32, No.6, pp. 1008- 1016, 1994.

Yang, J.Y. R.D. Spencer, T.M. Gates. 1995. *Analytical Solutions for Determination of Non-Steady-State and Steady-State Capture Zones.* Ground Water Monitoring Review. Winter. 101-106.

APPENDIX A

FINAL REMEDIATION DESIGN

(Group Project Summary, Results and Conclusions)

Summary

This appendix covers the technical aspects of the current situation of the Chemical Spill 4 (CS-4) groundwater plume at the Massachusetts Military Reservation (MMR), and proposes a final remedial design.

The aquifer underlying the MMR is contaminated by various pollutants forming a plume. The CS-4 plume is currently contained using a pump and treat system. The contaminants of concern detected in CS-4 are perchloroethylene (PCE), trichloroethylene (TCE), 1,2-dichloroethylene (DCE), and 1,1,2,2-tetrachloroethane (PCA). Granular activated carbon (GAC) is used to treat the extracted groundwater which is reinjected to the aquifer after treatment. This system was designed as an interim remedial action to quickly respond to the plume migrating off site. A final remedial design must be formulated.

In order to propose a final remedial system for CS-4, the following aspects are examined in depth: (1) an extensive site characterization, (2) the development of a computer model to simulate flow and contaminant transport, (3) the evaluation of the feasibility of bioremediation and its design, (4) the examination of the current aboveground treatment system and possibilities of its enhancing it; and (5) an evaluation of the risk associated with these remedial strategies.

Site characterization was based on previous studies of the area. Equilibrium sorption, however, was tested in the laboratory since this factor may affect the fate and transport of the contaminants. A three-dimensional model was constructed from the results of the site characterization. The model was used to simulate flow and transport under natural conditions, and to predict effective capture curves for the extraction of the contaminated water. An innovative in situ bioremediation system consisting of an anaerobic zone sequenced by an aerobic zone was designed. The removal due to

biodegradation was calculated. Optimization of the currently operating treatment system was conducted by evaluating economic benefits of combining the existing GAC system with zero-valent iron technology. Risk assessment was performed considering EPA acceptable range of carcinogenic and non-carcinogenic risk.

RESULTS

Site Characterization

Equilibrium Sorption

Sorption of contaminants by aquifer solid matrices significantly affects their fate and transport. The bioavailability of contaminants can be reduced considerably because of sorptive uptake. Also, remediation times can be prolonged substantially because of a continuous feeding of contaminants to the aquifer by the sorbed species. Another effect of sorption is that it may alter the dispersive behavior of contaminants (i.e., enhancement of longitudinal dispersivity).

One way to quantify all of these effects is to use equilibrium sorption distribution coefficients to calculated retardation factors. Laboratory batch tests are setup to determine distribution coefficients. These are used to validate the use of equilibrium relationships to extract retardation factors. Once this relationship was shown, (see Khachikian, 1996), retardation factors were calculated which were then used to assess the behavior of contaminants.

Equilibrium Sorption Results

The sand samples used in this study were obtained from the USGS Well S315 (Figure A-1)

The organic carbon content (f_{oc}) of the sands used in this study are listed in Table A-1. The f_{oc} is the part of the solid matrix primarily responsible for sorption.

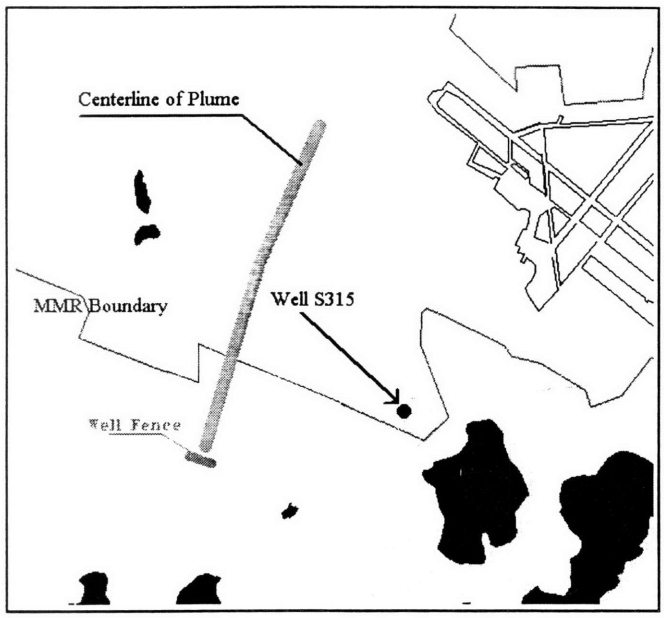

Figure A-1. Location of Well S315 relative to the centerline of the CS-4 plume, the base boundary and the current location of the extraction well fence.

Table A-1. Sand Identification including laboratory measured f_{oc}s and hydraulic conductivities, *K*. Samples were obtained from Well S315

Sand ID	Sand Depth (feet)	f_{oc} (±σ), (%)	K, cm/s[a]
S315-5	18-20	0.0433 (0.0015)	0.012
S315-13	58-60	0.0098 (0.0005)	0.041
S315-2	73-75	0.0058 (0.0013)	0.100
S315-14	78-80	0.0048 (0.0008)	0.060
S315-9	88-90	0.0076 (0.0011)	0.037

[a] The K values approximated from Figure 4.8.5 of Thompson (1994).

Using these f_{oc} values, equilibrium distribution coefficients are calculated (Table A-2). The f_{om} values listed in Table A-2 are assumed to be twice the measured f_{oc} values (Schwarzenbach et al., 1993). Phase partitioning is assumed as the predominant mechanism controlling sorption. Verification of this assumption can be found in Khachikian (1996).

Table A-2. K_d' values calculated from the linear equilibrium sorption equation $K_d'=K_{om}f_{om}$.

	K_d' (L/kg)			
Sample ID	f_{om}, %	DCE	TCE	PCE
S315-5	0.0866	0.026	0.063	0.158
S315-13	0.0196	0.006	0.014	0.036
S315-2	0.0116	0.004	0.008	0.021
S315-14	0.0096	0.003	0.007	0.017
S315-9	0.0152	0.005	0.011	0.028

Implications of Distribution Coefficients

In this section, the implications of sorption on field-scale contaminant transport is discussed.

Effects of Sorption on Contaminant Transport

The depth-averaged retardation factors calculated for the contaminants of interest were calculated (Table A-2). Khachikian (1996) describes retardation factors in more detail.

Table A-3. Effective retardation factors

Compound	R_{eff}
DCE	1.04
TCE	1.10
PCE	1.25

The longitudinal macrodispersivity is a key factor in the modeling and understanding of plume transport. The value for the longitudinal macrodispersivity for a conservative substance at Cape Cod is estimated to be 20 m (66 ft) (Lázaro, 1996). However, for sorbing solutes, an adjustment to this value has to be made. The net effect of sorption is to retard the transport (i.e. the velocity) of the contaminants in the aquifer. Variability of sorption can produce an enhanced longitudinal macrodispersivity (Garabedian et al., 1988); this effect is more important when the sorption coefficient and hydraulic conductivity are negatively correlated (Figure A-2).

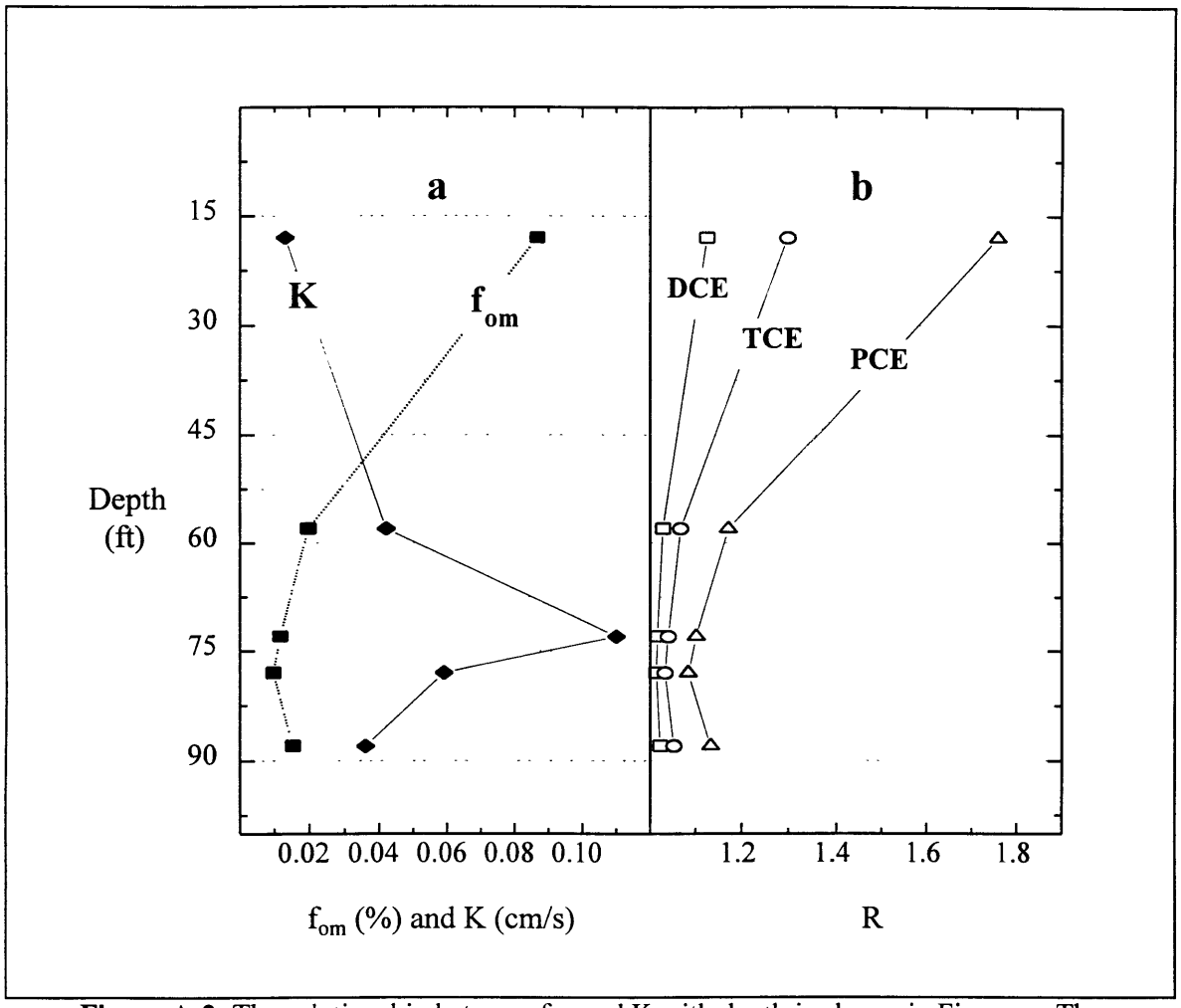

Figure A-2. The relationship between f_{om} and K with depth is shown in Figure a. The experimentally determined retardation factors are shown in Figure b. As expected, the f_{om} and K and the R and K are inversely related.

The values of the retarded longitudinal macrodispersivity, A_{11}, are included in Table A-4. For the more strongly sorbing PCE, the retarded longitudinal macrodispersivity, A_{11}, increases by a factor of 2.1 relative to the non-retarded value. This is an important consideration in the modeling or understanding of the transport of this compound. For the least sorptive compound (DCE), the velocity variances introduced by sorption are small as reflected by a small increase in the longitudinal macrodispersivity (factor of 1.2).

Table A-4. Values of the retarded longitudinal macrodispersivity, A_{11} (Khachikian, 1996).

Compound	A_{11} (m)
DCE	23.5
TCE	28.7
PCE	41.3

The retarded longitudinal macrodispersivity, in effect, quantifies the extent of a mixing zone in front of the leading edge of a contaminant plume. While the bulk of the mass of the contamination may be held back (i.e., retarded), some will disperse ahead of the conceived contaminant plume, resulting in early breakthrough times.

Macrodispersivity is a phenomenon that is currently under research. The effects are scale dependent and, thus, presents a certain challenge to the investigator. More research is needed to fully understand this phenomenon and to be able to quantify it.

Contaminant Transport Modeling

Description

A particle tracking code was used to simulate the movement of particles from the source for a specified amount of time. Particle locations were recorded at the end of each simulation and concentrations were calculated based on particle weight and number of particles per unit volume. A more detailed description of some aspects and outcomes of the transport model is discussed next.

Source

A thorough description of the source, its location, dimensions, and input loadings are essential for a reliable model. E.C. Jordan (1989b) provides a thorough description of what is believed to be the CS-4 plume source.

The transport model focuses on the solvents PCE, TCE and DCE. Due to limitations in the program code, they were modeled as one contaminant. Thus,

concentration outputs files included the sum of PCE, TCE, and DCE concentrations. The source loading was calibrated to match the field values. Consequently, the calculated concentrations are compared to the observed values at different well locations.

The source was modeled as a continuous source input. From groundwater velocity data, it was determined that the contamination must have started at least 15 years ago. The source loading was modeled as seven 5 year intervals, from 1960 to 1993 (Figure A-3).

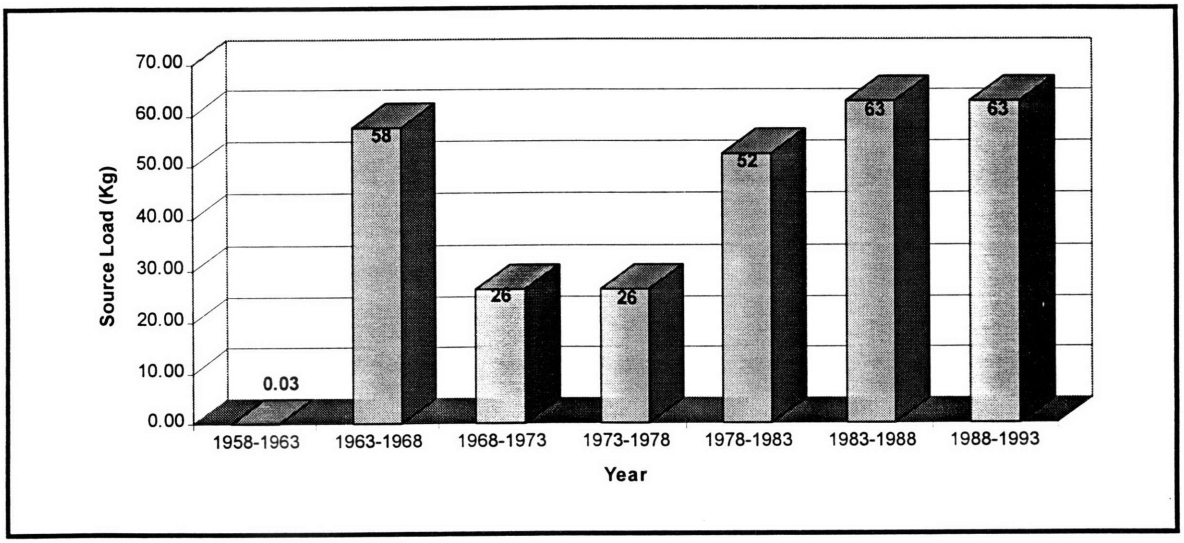

Figure A-3: Source Loadings for the CS-4 Model

Dispersivity

Garabedian et al. (1988) calculated dispersivities using the data obtained during the Ashumet Valley tracer test. The method of spatial moments was used to interpret the data; which was regarded by Gelhar et al. (1992) as having a high degree of reliability. Values of dispersivity obtained by Garabedian et al. (1988) are summarized in Table A-5 below.

Table A-5. Dispersivity values of the Ashumet Valley Tracer Test (*Garabedian et al.*,1988)

Dispersivity	Value
Longitudinal (A_0)	3.15 ft
Transverse, horizontal (A_{22})	0.59 ft
Transverse, vertical (A_{33})	0.005 ft

It must be noted that these values, which are generally well accepted in the literature for the site, were obtained for a source with different dimensions as the CS-4 site. The displacement of the CS-4 plume is larger than that of bromide used in the tracer test experiment. Consequently, the overall test scale of the CS-4 site is larger, and the macrodispersivity should be modified (Gelhar, 1993). In addition, Rajaram and Gelhar (1995) conclude that dispersivities for transport over large scales are significantly influenced by the source dimensions. The authors define a relative dispersivity which are is appropriate for characterizing the dilution and spreading at individual heterogeneous aquifers. Using their two scale exponential model, the relative longitudinal dispersivity (A_0^r) is estimated to be 20 m (66 ft) (Gelhar, 1996).

Transverse dispersivities are not affected, since their variability is not due to this phenomenon but to temporal variations of the hydraulic gradient's direction (Rehfeldt and Gelhar, 1992). This is a topic that is undergoing current research, and thus is beyond the scope of this work.

Transport Model Results

The code's capabilities allow concentration contours to be delineated. From this information the general size and shape of the contaminant plume was evaluated. The figures below (Figures A-4 to A-6) show the graphical output of the model.

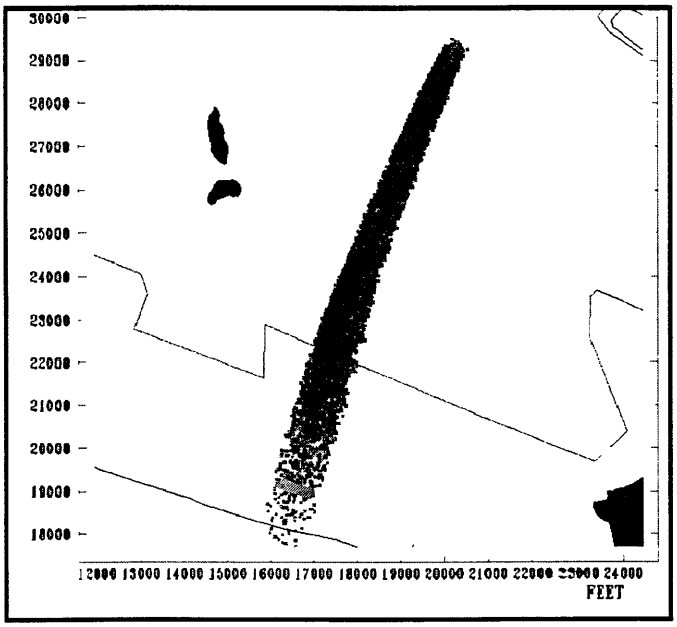

Figure A-4: Distribution of Particles in the CS-4 Plume Simulation

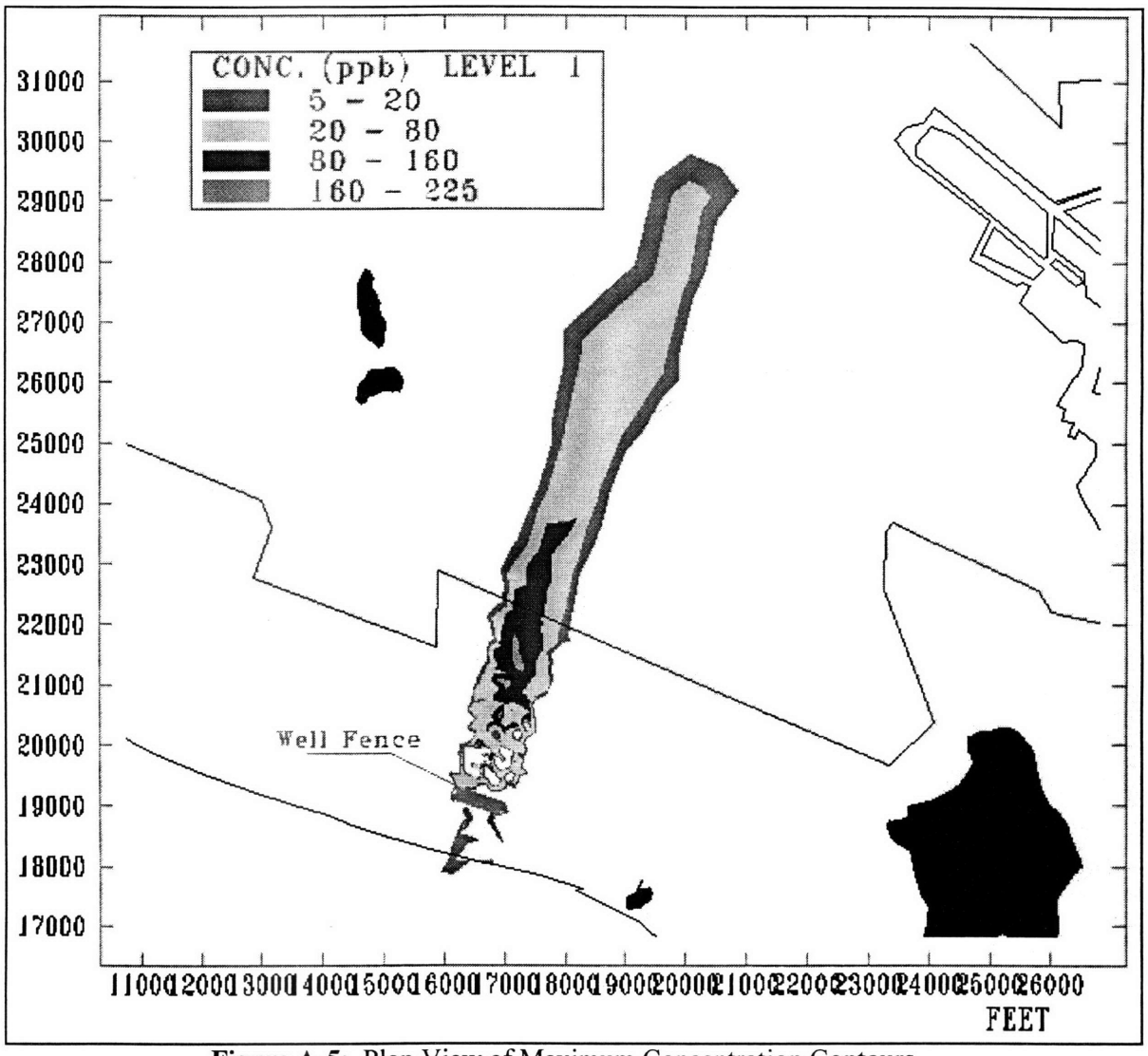

Figure A-5: Plan View of Maximum Concentration Contours

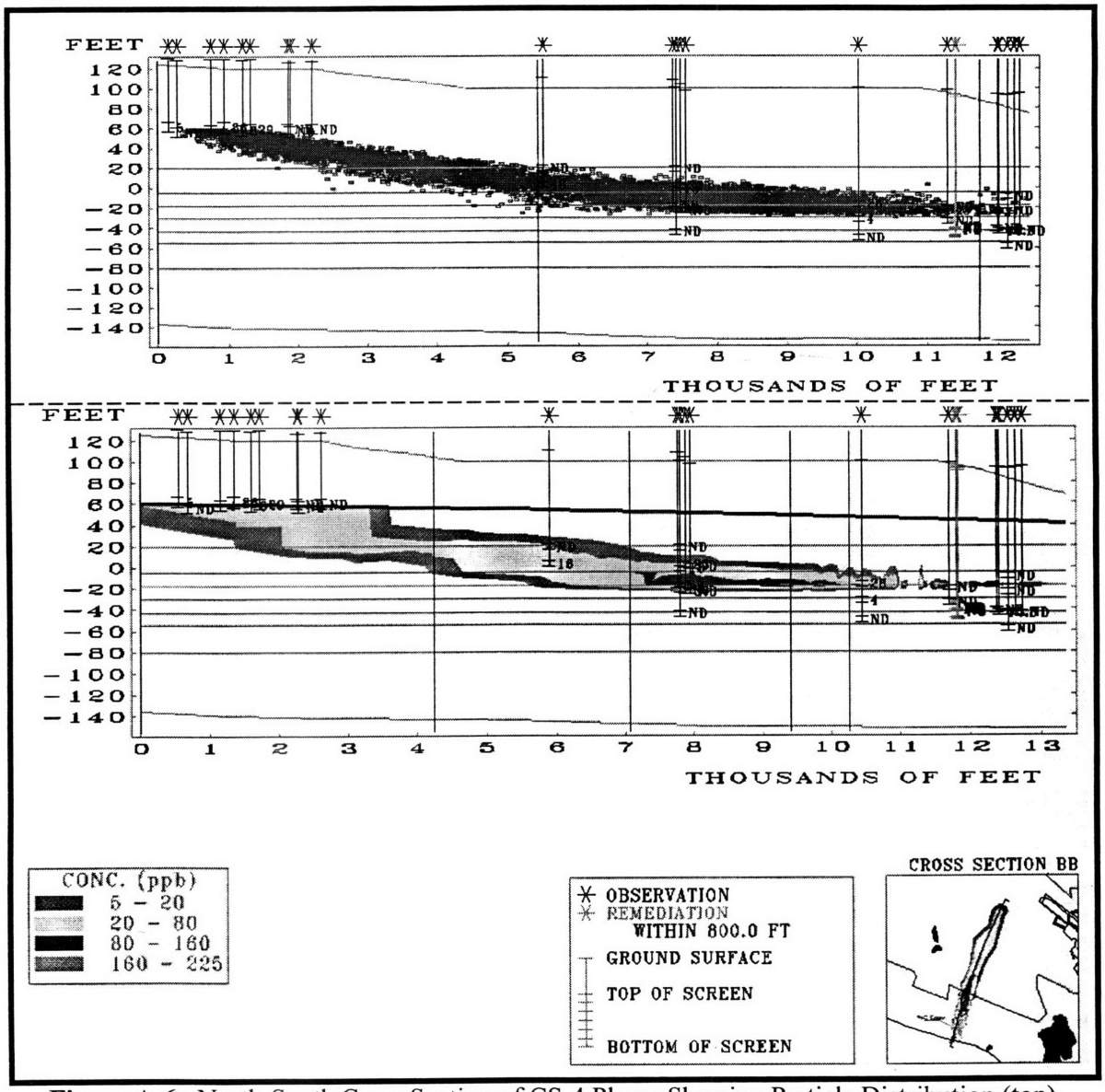

Figure A-6: North-South Cross Section of CS-4 Plume Showing Particle Distribution (top), Concentration Contours (bottom)

In general, the dimensions of the modeled plume (Table A-6) are greater than the ones reported by ABB Environmental Services (1992b). This result does not necessarily invalidate either plume interpretation. The plume defined by ABB Environmental Services Inc. (1992a) was developed from interpretation of the field observations. This simulation used field observations and site characterization data, applied to a calibrated

natural conditions model of the Cape Cod aquifer, and thus probably produces a more appropriate representation of the real plume. Nevertheless, there are many assumptions that are made and factors that come in when a computer model is constructed. Some of these, such as source dimensions and location, recharge, hydraulic conductivity distribution, amount of data available; may ultimately be the sources of discrepancy between the modeled solution and the real plume. This suggests that site characterization should be improved in order to obtain a clearer understanding of the subsurface conditions.

Table A-6: Dimension of Modeled Plume

arameter	alue
ength	2,600 ft
aximum Width	,100 ft*
verage Width	,180 ft
aximum Height	5 ft
verage Height	0 ft

* *Maximum width is probably overestimated due to grid resolution*

Transport Simulations

The CS-4 plume model described above was used to simulate two different remediation alternatives. Both simulations were started with the plume as shown in Figure A-6 (in the simulation year 1993). These simulations attempted to forecast the clean-up times for the alternatives examined. A detailed description of the simulations is included in Lázaro (1996).

The first simulation was the no action alternative and therefore modeled the natural flushing of contaminants. Assuming that the source of contaminants was eliminated in 1993, the total time it took for all the particles to enter Coonamesett Pond was between 80 to 85 years. Thus, the model suggests that if the well fence had not been

operating, the aquifer under the MMR would be "clean" approximately by the year 2075. Once the particles reached the pond, concentrations dropped notably, possibly due to dilution effects. This model could be used as the basis for further studies on surface water impacts.

The second simulation attempted to replicate the current pump and treat scheme used at the MMR. Thirteen extraction wells at the toe of the plume pump at a total rate of 140 gpm. The purpose of the simulation was to predict the time it would take to operate the pump and treat system continuously until concentrations reach acceptable levels. This occurred approximately 70 years after the simulation run started. This strongly suggests that a more economically efficient final remediation scheme should be put in place.

Bioremediation

General Considerations

In bioremediating a site, the engineering of the delivery systems and their control present the engineer more challenge than understanding the biochemical process. The main problem with traditional applications of in situ bioremediation is that the delivery of the added agents is in the liquid form resulting in displacement of the contaminated water and therefore inadequate mixing. This results to minimal biodegradation.

To overcome this problem, all agents of choice are added in the gaseous form. The injected gases move through the aquifer in discrete channels (Hayes, 1996) diffusing into the water on their way to the surface (carried by buoyancy). This creates a continuous source of the injected agent in the water.

Cometabolic Oxidation and Reductive Dechlorination

Xenobiotic compounds (i.e. foreign to natural biota) such as the chlorinated solvents found at the CS-4 site cannot be utilized by microorganisms for growth and energy (Nyer, 1992). The process of aerobic cometabolic oxidation has been proven to biodegrade TCE and other aliphatic compounds. Methane-oxidizing microorganisms

have been found to be capable of cometabolically oxidizing TCE, DCE, and vinyl chloride (VC) in aerobic environments (Semprini et al., 1991a).

PCE, however, can only be removed in anaerobic environments in a process termed reductive dechlorination. In this process, PCE loses a chlorine atom (turning into TCE) and achieves a lower oxidation state becoming susceptible to cometabolic oxidation.

Process Design

A successful bioremediation scheme for CS-4 should consist of an aerobic phase (for the treatment of TCE and DCE) and an anaerobic phase (for the treatment of PCE). This design was incorporated in three phases.

Horizontal wells were utilized to inject the gases. Horizontal wells are advantageous over vertical ones because they can extend along a wide plume replacing up to 10 wells (Parmentier and Klemovich, 1996). The area of influence of the injected gases creates a biozone where the treatment takes place. It was assumed that a methane concentration of 1 mg/L and DO concentration of 10 mg/L can be achieved in the biozone.

A pilot field test conducted at another site formed the modeling basis of the aerobic cometabolic part of the system design at CS-4 (Semprini and McCarty 1991b, Semprini and McCarty 1992a). The reductive dechlorination estimations were based on laboratory studies as discussed by Collins (1996).

Phase 1

The objective of phase 1 was to stimulate microbial growth by injecting methane, air, and nutrients so a steady-state methanotrophic biomass (SSMB) concentration was reached.. Once SSMB was reached, phase 2 begins. It was calculated that it took about 5 days to create a SSMB of 5 mg/L.

Phase 2

Phase 2 was an anaerobic phase. Its objective was the removal of PCE. The SSMB created in phase 1 was required as the electron donor in phase 2. To create an anaerobic environment, the injection of methane and nutrients was continued while the injection of air was stopped. This exerted a biochemical oxygen demand to the aquifer turning it anaerobic in. The DO carried into the biozone by the water was consumed in just 2 ft. Collins (1996) calculated that under these conditions a 99 % removal of PCE can be achieved if adequate residence time is allowed. Degradation of PCA but can not be quantified due to lack of relevant previous studies. The residence time can be increased by the addition of horizontal wells which will extent the biozone by 200 ft per well. This corresponds to a residence time of 250 days per well since the seepage velocity is 0.8 ft/d (Lázaro, 1996).

Phase 3

Biozone II was placed downstream at a distance where no interference with biozone I would be possible (about 300 ft). In phase 3, methane and air were injected into the subsurface to stimulate cometabolic oxidation of TCE, DCE, and VC (VC be a by-product of phase 2). The resulting normalized concentrations of the contaminants are shown in Table A-7.

Table A-7. Resulting normalized concentration of TCE, DCE, and VC

	TCE	c-DCE	t-DCE	VC
k_{deg} (d^{-1})	0.014	0.068	1.36	1.36
t (d)	250	250	250	250
Cc/Cc_o	0.03	0	0	0

Figure A-7 shows the degradation of the contaminants within the biozone as a function of distance.

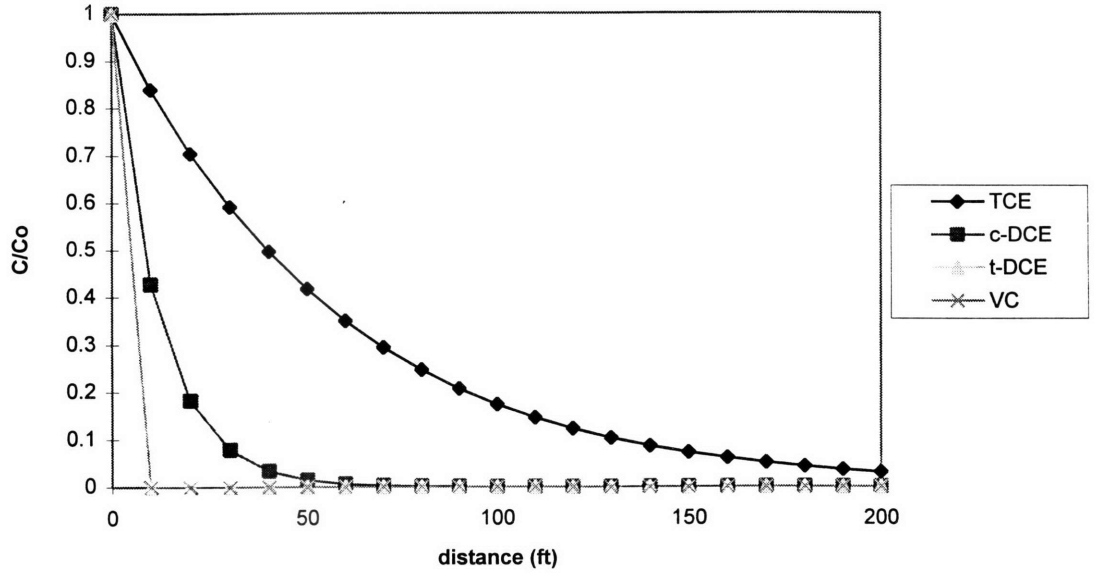

Figure A-7. Normalized contaminant concentrations as a function of distance

Discussion

A 97% removal of TCE, 99 % removal of PCE, and complete removal of the rest of the contaminants was achieved by this scheme. The conditions required (1.0 mg/L methane aqueous concentration and 10.0 mg/L) were assumed to be achievable in the field through proper engineering measures.

Field conditions are complex and hard to control. Factors affecting the in situ bioremediation of contaminants vary from site to site and caution must be given in the interpretation of the results obtained in this design. The contaminant removal calculated must serve for estimation purposes only. The mass transfer limitations and the spatial heterogeneity encountered at a site create conditions that cannot be adequately predicted by theoretical approaches. A pilot test is necessary to predict the system's efficacy and determine final design parameters.

Aboveground Treatment Alternative

It has been shown that the use of zero-valent iron is highly effective in promoting the breakdown of halogenated organic compounds in aqueous solution (Gillham, 1995). It was examined whether this emerging zero-valent iron technology could be combined cost-effectively with the existing GAC (Figure A-8). And whether this combination would be a feasible implementation at the CS-4 site.

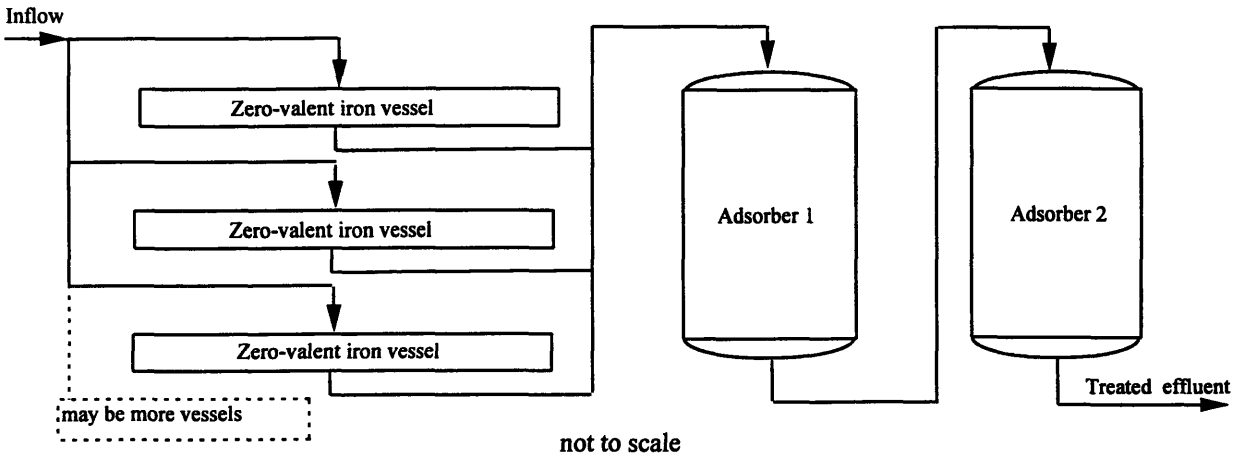

Figure A-8. Combination of zero-valent iron with GAC

The basic concept is to pass the contaminated water through vessels filled with granular zero-valent iron before passing it through the GAC. The contact of the VOCs with the iron surface results in reductive dechlorination and thus destruction of the contaminants. Since this technology is innovative and only very little data regarding the efficiency and implementability is available, the GAC is added to the system as a polishing and safety unit. As a result of degrading the contaminants before they enter the GAC columns, the carbon does not get exhausted and therefore carbon reactivation costs can be reduced. Assuming the innovative zero-valent iron technology is feasible, a comparison between investment and savings indicates the worth of the concept. For a detailed discussion see Tillman (1996).

Scenarios of inflow concentration

The size of the treatment facility depends on two major parameters: volumetric flowrate of water and the range of inflow concentrations of contaminants to be treated.

Since only about 20 samples determine the range of contaminant concentrations, the uncertainty is large. Furthermore, the proposed bioremediation system (previous section) has never been tested in the field and therefore its efficacy as a treatment scheme is uncertain. In order to understand the behavior of the treatment system with respect to different inflow concentrations, the following calculations were made for four different scenarios. The four scenarios are thus defined as follows and summarized in Table A-8 (see Table 2.4 for concentrations):

Scenario 1: Assuming the maximum concentrations in the influent and bioremediation was not capable to diminish plume concentrations This scenario represents the worst case.

Scenario 2: Assuming average concentrations prevailed throughout the whole plume, and no reduction by bioremediation.

Scenario 3: Assuming that bioremediation reduced plume concentration, which were initially taken as maximum concentration.

Scenario 4: Assuming that bioremediation reduced plume concentrations, which were initially taken as average concentration.

Table A-8. Four scenarios for influent concentrations

Contaminant of concern	Scenario 1: max conc. no bioremediation (ppb)	Scenario 2: average conc. no bioremediation (ppb)	Scenario 3: max. conc. with bioremediation (ppb)	Scenario 4: average conc. with bioremediation (ppb)
PCE	62	18	0	0
TCE	32	9.1	0	0
1,2-DCE	26	1.1	0	0
1,1,2,2-PCA	24	6.8	24	6.8

Combination of abiotic dehalogenation and GAC

The net savings depend on the influent concentrations (Table A-9). For high concentrations (scenario 1), considerable savings can be expected, while at lower inflow

concentrations (scenario 2-4), the costs are higher than the savings. Calculations are shown in Tillman (1996).

TableA-9. Net savings of the combination of GAC and zero-valent iron

Scenario	Costs: Installation of zero-valent iron system and reduced carbon exchange cost (million $)	Savings: Present worth of carbon exchange cost (million $)	Net savings (million $)
Scenario 1	0.4	0.6	0.2
Scenario 2	0.2	0.3	0.1

The results do not allow firm conclusions but require appropiate interpretation. Some assumptions made for the calculations are the following: steady inflow concentration, multi-component adsorption prediction, half-lives of the reductive dechlorination process, build-up of by-products, cost of the iron technology (vessels, construction etc.) and project lifetime. Therefore, the net savings should be seen as an order of magnitude estimate.

Conclusions

The results indicate that the combination of GAC with zero-valent iron could be feasible and result in a more economic aboveground treatment than the existing one. Furthermore, in the near future the iron process is expected to progress significantly (Gillham, 1995). In order to better determine the effectiveness of this system, more data is required. A better estimation of the actual plume contamination and bench-scale or pilot testing of the zero-valent iron technology for the CS-4 site specific parameters are needed.

Risk

Introduction

In the CS-4 plume, four hazardous substances are identified as primary contaminants in the groundwater: PCE, TCE, DCE and PCA. Both carcinogenic and non-carcinogenic health effects are associated with these chemicals.

Results

In the bioremediation scheme two cases are presented because the amount of PCA that is degraded cannot be estimated due to lack of data. Two cases are then applicable: one wherein all PCA is degraded, and one where all the PCA remains in the groundwater. PCA is more likely to be degraded, and a pilot study will be useful to determine the level of PCA degradation. Table A-10 shows the resulting concentrations.

Table A-10. Contaminant levels after cleanup through bioremediation

	µg/L	PCE	TCE	DCE	PCA
Case 1	Maximum	0.6	1	0	0
	Average	0.2	0.3	0	0
Case 2	Maximum	0.6	1	0	24
	Average	0.2	0.3	0	6.8

In the case where PCA may not be subject to bioremediation, as mentioned above, a pump and treat system is necessary to remove the PCA. In this case the resulting contaminant concentrations are tabulated below (Table A-11).

Table A-11. Contaminant levels after cleanup through bioremediation and pump and treat

µg/L	PCE	TCE	DCE	PCA
Maximum	5	5	0	2
Average	5	5	0	2

Table A-12 summarizes the risks associated with the different treatment schemes. The data contained in the table can be viewed graphically in Figures A-9 and A-10. Both the table and the graph show that, following EPA guidelines, the plume must be

remediated. Since it is possible to almost completely remove all contaminants from the groundwater, the best case for all remediation strategies involves no risk.

Table A-12. Risks associated with remediation schemes

	Carcinogenic Risk		Non-carcinogenic Risk	
	Maximum	**Average**	**Maximum**	**Average**
no action	1.6×10^{-4}	4.5×10^{-5}	3.7×10^{-1}	9.2×10^{-2}
pump and treat	1.4×10^{-5}	1.4×10^{-5}	9.5×10^{-2}	3.8×10^{-2}
bioremediation (1)	3.1×10^{-7}	8.9×10^{-8}	5.7×10^{-3}	1.6×10^{-3}
bioremediation (2)	1.5×10^{-4}	4.2×10^{-5}	5.7×10^{-3}	4.5×10^{-3}
combination (bio 2)	1.3×10^{-5}	1.3×10^{-5}	5.7×10^{-3}	1.6×10^{-3}

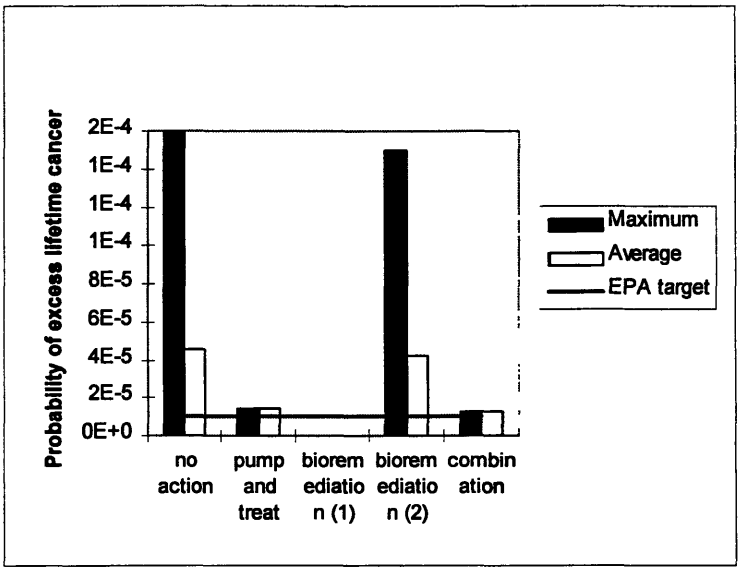

Figure A-9. Carcinogenic risk

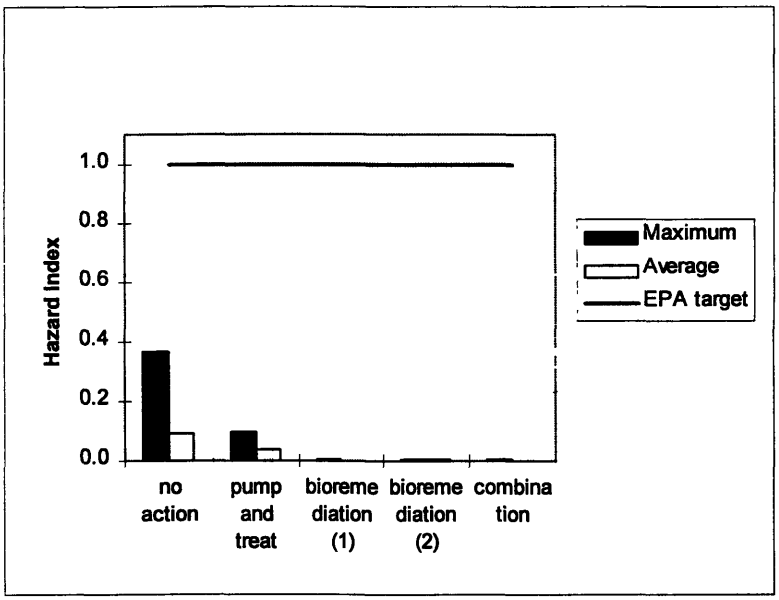

Figure A-10. Non-carcinogenic risk

Discussion

The process of calculating risk involves the use of approximations and conservative assumptions. Thus the risks calculated are generally estimates. Keeping in mind that the primary purpose of risk assessment in this project is the comparison of alternative remediation strategies, these values then become meaningful. All the uncertainties inherent in the calculations apply to each remediation scenario, and therefore the risks can be compared across remediation strategies. The assessment can also show which of the contaminants poses the greatest risk. It is apparent that simply allowing the plume to proceed unabated can result in unacceptable risk, at least from a regulatory standpoint. In addition, the calculated risks do not take into account any potential ecological risk if groundwater contaminants are discharged into surface waters such as Coonamessett Pond. From Figure A-9 it can be seen that all calculated non-carcinogenic risks are well below the Hazard Index limit of 1.0, and do not seem to pose a threat to human health. Carcinogenic risks, however, vary up to two orders of magnitude from case to case. Figure A-10 shows that in contrast to non-carcinogenic risks, carcinogenic risks for the no action alternative are above the limit. The various treatment schemes yield risks within acceptable range, except for the bioremediation case where PCA is assumed to

resist degradation. In this case a pump and treat system is necessary to remove PCA. From a risk point of view, any of the alternatives which reduce the risk to permissible levels is acceptable. Therefore the pump and treat system, the bioremediation scheme (assuming satisfactory PCA degradation), and a combination of the two are acceptable. However, the one which realistically yields the lowest risk, namely the combination, is the recommended one. The bioremediation scheme which assumed complete PCA removal results in the lowest calculated risk, but if this is true then addition of pump and treat system will lower the risk even more. Aside from the lowered risk, the pump and treat system serves as a back-up to the bioremediation, especially during the start-up period. The combination assures the satisfactory removal of the groundwater contaminants. It should be noted that the incremental risk of developing cancer is minute compared to the background cancer risk of 0.25. Aside from this, the likelihood that a well will be installed in the vicinity of the plume is small. Despite this, the public perception is that this level of increased threat of cancer is unacceptable, and therefore the water must be cleaned up and the threat removed.

Conclusion

This project was undertaken to fully understand the transport mechanisms of groundwater and contaminants in the western Cape Cod aquifer, and to develop a final remediation scheme for the CS-4 plume. The following conclusions are drawn:

- Site characterization must be improved in order to provide a clearer understanding of the contamination problem. The representation of the aquifer conditions with the computer model was limited because of insufficient data.
- Total clean-up times using the current interim remedial scheme are very long and cost intensive. Development of a final remediation method which decreases clean-up times and decreases costs is necessary.

- Using only seven of the 13 existing wells produces the same results as the current operation. Reexamination of the current pumping scheme would reduce operation and maintenance costs. It is recommended that this new scheme be examined as an alternative to the existing operation.
- The anaerobic/aerobic in situ bioremediation scheme proposed demonstrates that it has the potential to completely degrade PCE, TCE, and DCE. A pilot test is needed to demonstrate the efficacy of this technology and determine the final design parameters.
- By combining the existing GAC with the emerging zero-valent iron technology a reduction in overall treatment costs can be achieved for certain scenarios. A bench-scale study should be conducted to verify the results.
- Risk calculations indicate that the CS-4 plume must be remediated to comply with regulations. The remediation strategies reduce the risks to acceptable levels. From a risk standpoint, the preferred strategy is a combination of bioremediation and pump and treat.

APPENDIX B

Natural Flow Model Calibration

A. Sensitivity Analyses

For the sensitivity analyses of the model, in which sensibility to recharge and boundary conditions and hydraulic conductivity were changed, the results showed an important influence of the hydraulic conductivity in the head distribution throughout the aquifer. The influences of recharge changes or the release of the heads at the shorelines of Ashumet and Johns ponds, were not important in the overall flow in the aquifer. The variations in the error and standard deviation due to changes in recharge and type of boundary conditions are presented in Table B-1.

In the case of the recharge, the distribution of error in the modeled area remained the same. The general flow was not disturbed when recharge was varied. When the type of boundary condition was changed from fixed head to free head at Ashumet and Johns pond shorelines, the flow experimented a slight change near the ponds. The different error and standard deviation due to these changes was, in general, due to the changes in heads near these ponds. However, as can be seen in Table B-1, the variation in the error was minimum, and the flow in the CS-4 area was not perceivably modified.

Table B-1. Mean error and standard deviation for the sensitivity analysis. Recharge in the modeled area, and boundary conditions at Ashumet and Johns ponds were tested.

Simulation	Model Conditions	Mean Error	Standard Deviation
Calibrated Model	Recharge = 23 in/yr, and Heads fixed at Ashumet and Johns Ponds	-0.214 ft	1.255 ft
Recharge Sensitivity	26 in/yr	-0.235 ft	1.304 ft
	19 in/yr	-0.219 ft	1.278 ft
Boundary Conditions Sensitivity	Free heads at Ashumet and Johns Ponds	-0.296 ft	1.075 ft

According to these results, heads in Ashumet and Johns Ponds were maintained fixed during the calibration and simulation procedures. Recharge, in turn, was set to 23 inches per year and maintained at that value. Hydraulic conductivity was the parameter to vary for the calibration procedure. The anisotropy ratio was also kept constant for the regional, no-stress flow model calibration, since flow in the aquifer is predominantly horizontal.

B. Calibration

The calibrating parameter was the horizontal hydraulic conductivity. Values of this parameter were changed in many different ways, maintaining always the trends described in Masterson and Barlow (1994) discussed in Section 3.3.1. Head contours interpolated as described in the methodology proved to be useful as initial targets for rough calibration, since it was easier to visualize and therefore calibrate to head contours than it is to heads at specific points. The final calibration criteria, however, were based on point values. From the head contour comparison, the most notable differences were the effects of ponds and streams on the groundwater flow. Refinement of the grid was necessary in the pond areas to accurately represent them using the high hydraulic conductivity values and, thus, have the desired effect.

After these adjustments and further variation of the hydraulic conductivity, the model approximated the target values fairly well throughout the outwash plain. The model was considered calibrated after reaching a mean difference of -0.214 ft in head and a standard deviation of 1.255 ft. for the entire region. Also, positive and negative errors should be equally distributed in the area of interest. However, in the moraine, values do not converged to the target values as well. A definitive effect of the moraine properties on the overall head pattern was evident and hydraulic conductivities in the moraine had to be revised to adjust the head as best as possible.

In the moraine region, the calculated heads seem to be higher than the observed head. In the CS-4 area, however, the error was minimal and well distributed. In order to decrease the error in the moraine, hydraulic conductivity was changed in many different ways making use of the vertical distribution of materials assigned to this region.

However, as mentioned above, changes in the moraine clearly affected the flow pattern in the CS-4 area. In Ashumet Valley, calculated heads tended to be lower than the observed ones. As in the case of the moraine, this error was corrected as much as possible and the remaining error was considered not important for the modeling purposes in CS-4.

In Figure 3.2, the distribution of hydraulic conductivity is presented. The average groundwater pore velocity can be calculated using the Darcy Equation

$$v = \frac{K}{n_e} J$$

where, v= average groundwater pore velocity

K= hydraulic conductivity

J= hydraulic gradient

n_e= effective porosity

To compute velocity, the value of 0.39 for effective porosity is used. For hydraulic conductivity it is convenient to consider only the area of CS-4 plume and take the arithmetic mean of hydraulic conductivity of the lithologic facies in which the plume moves. It is necessary to calculate the average of the upper-most layer thickness since this is not constant. The calculated arithmetic mean for the area in which the plume is located is:

$$K_h = \frac{(120\,ft/day)(50\,ft)+(217\,ft/day)(140\,ft)}{50\,ft+140\,ft}$$

$$K_h = 191\,ft/day$$

The hydraulic gradient resulting from the model, was 0.0014. Using the values for K, n_e, and J mentioned above, the average groundwater pore velocity is 0.67 ft/day.
The final hydraulic conductivity, anisotropy ratios, gradient, and velocity for the area of the CS-4 plume are presented in Table B-2.

The value of velocity in the area of CS-4 plume is lower than values reported in the literature (LeBlanc et al., 1991; Garabedian et al., 1991) of 0.4 m/d (1.3 ft/day). The reason for this may be that in the presented model, the northern part of the western cape is

not included, which has predominantly very high values of hydraulic conductivity (Masterson and Barlow, 1994) associated with the proximal sedimentary facies which are characterized by coarser grain size. Besides, the thickness of the coarse sand and gravel material corresponding to the shallow sediments increases as we go north. This makes the overall hydraulic conductivity increase as well. Since our modeled area is located in the southern part, we miss the higher conductivity values, obtaining a lower groundwater velocity.

Table B-2. Hydrogeologic parameters resulting from the groundwater flow model. Values correspond only to the CS-4 plume area.

Parameter	Value
Average Hydraulic Conductivity	191 ft/day
Gradient	0.0014
Velocity	0.67 ft/day
Anisotropy Ratio	3:1, 5:1 and 10:1

Aquifer Test Simulation

As mentioned in the methodology, head data from 7 single level monitoring wells and a multi-level well were available for the calibration of the model. In Figure B-2 we can see a plan view of the drawdown distribution and the location of the six nearest monitoring wells. In Figure B-3 the differences between the measured and the simulated drawdown are shown, in a cross-section. The final mean difference is -0.153 ft and the standard deviation is 0.185 ft.

This differences are important to decide if the model is calibrated in its anisotropy ratio. However, the shape of the ellipse formed by the drawdown contours, and the shape of the time drawdown curves, were consider just as important.

As described by Freeze and Cherry (1979), drawdown at any point at a given time is directly proportional to the pumping rate and inversely proportional to the aquifer transmisivity T and aquifer storativity S. For an ideal confined aquifer, the time-drawdown curve would be the ideal Theis curve, but the response of a real aquifer to

pumping often deviates from it, according to its geologic configuration. Thus, obtaining from the model a similar curve to the actual test curve, showing the same trends in different periods of time, was important to confirm the proper representation of the aquifer.

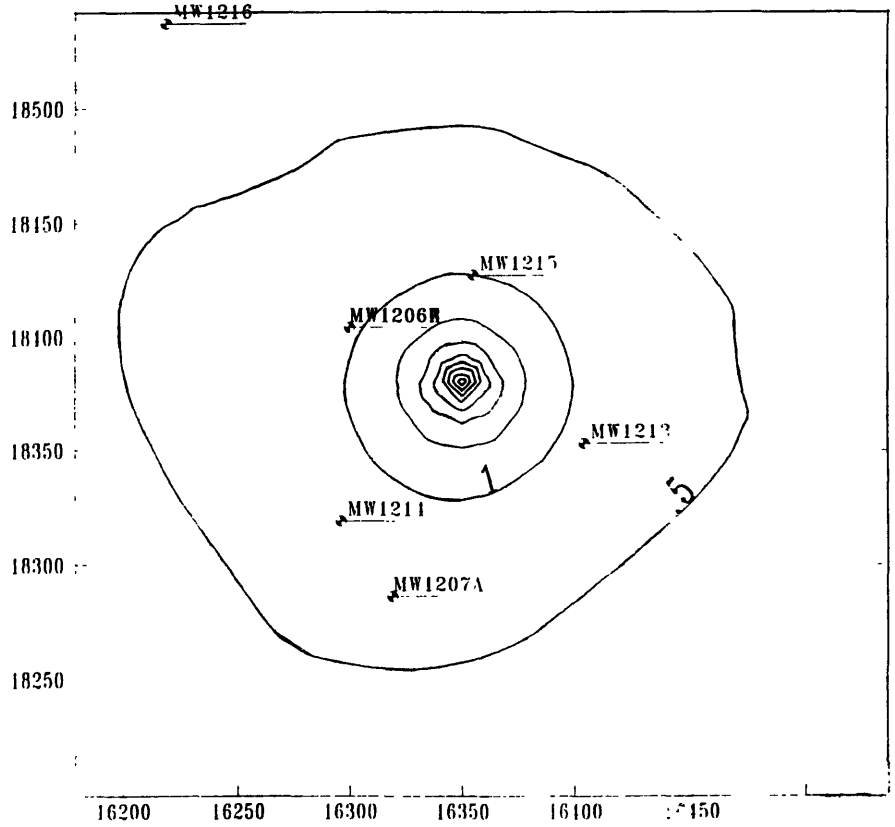

Figure B-2. Plan view of the drawdown distribution and location of monitoring wells.

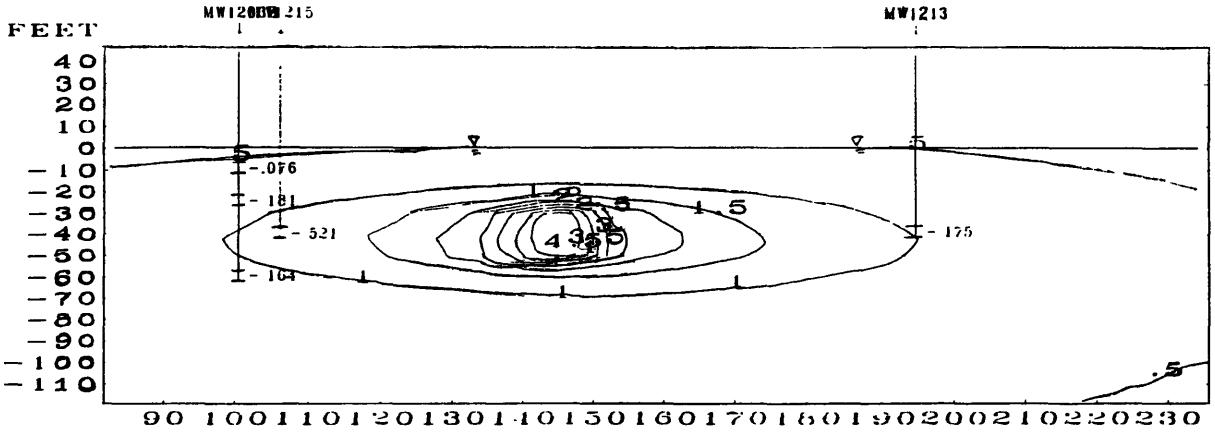

Figure B-3. Cross-section at the pumping well showing the drawdown distribution for the aquifer test simulation. The elliptical shape of the contours is due to the anisotropy.

The shape of the drawdown curves obtained from the simulations were similar to the shape obtained by real measurements in the field. An example of the drawdown obtained in the simulation is shown in Figure B-4. Figure B-5 shows the drawdown curve obtained in the actual pump test for the same well.

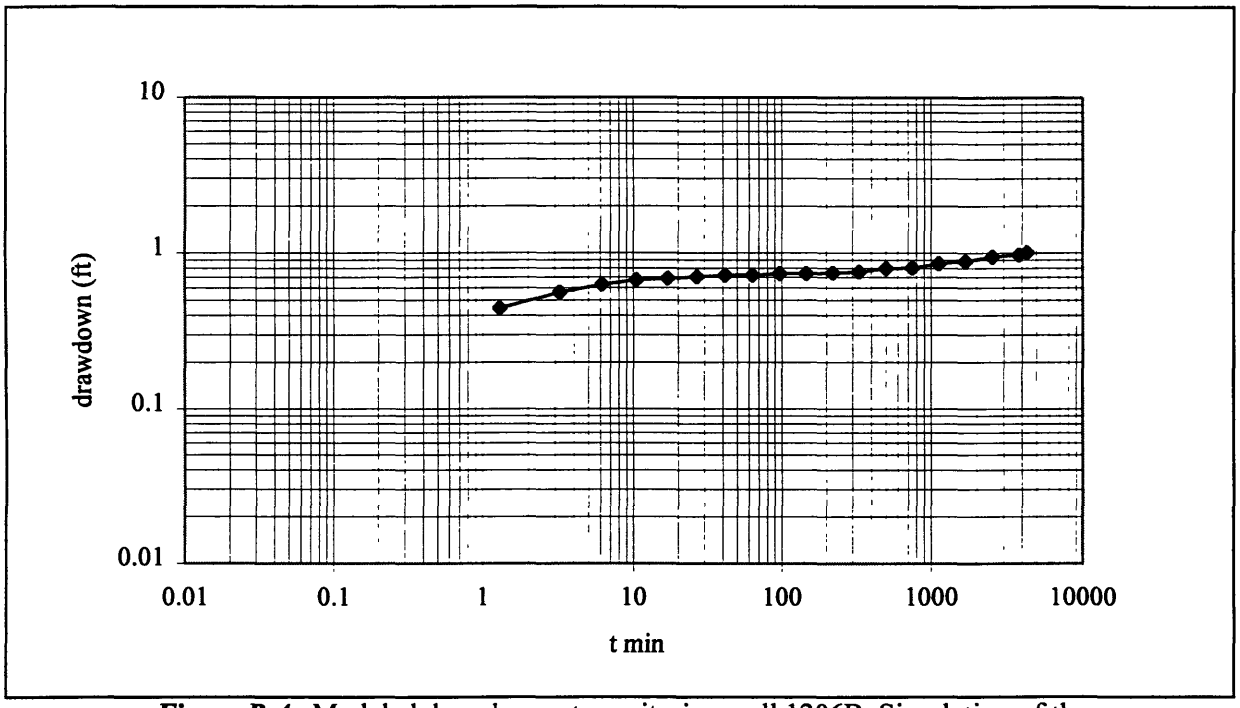

Figure B-4. Modeled drawdown at monitoring well 1206B. Simulation of the aquifer test performed at the CS-4 area by E. C. Jordan in 1989.

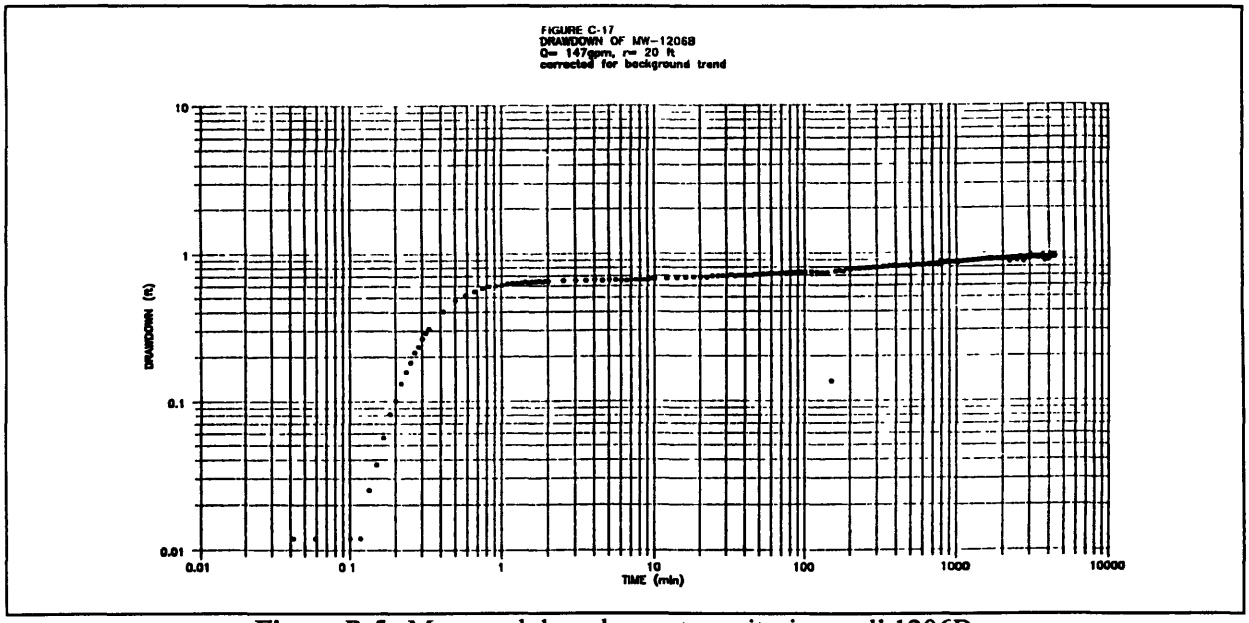

Figure B-5. Measured drawdown at monitoring well 1206B. Aquifer test performed at the CS-4 area by E. C. Jordan in 1989.

Based on the cross-section of drawdown presented in E. C. Jordan (1989), the ratio of minor and major axis of the ellipses were calculated giving a result of 0.41, while the simulated pumping test gives a ratio of ellipse-axis of 0.38 (calculated from the cross-section showed in Figure B-3). The anisotropy ratios giving the best results are 3:1 for the upper layers of medium-coarse sand and gravel, 5:1 to the middle layers of fine-medium sand, and 10:1 for the find sand and silt layers at the bottom of the aquifer. Specific storage was maintained at the value of 0.001 ft^{-1}.

APPENDIX C

MODELING INPUT AND COMMAND FILES

C-1. Site file

!SITE FILE FOR THE CS-4 MODEL

```
!
FEET FINISH
PLANMAP 1  XMIN  -23500.44  XMAX   40000.45 DELX   10000.00 &
        YMIN  -23500.00  YMAX   40200.00 DELY   10000.00 &
        XLL   .382  XUR   .970  YLL   .177  YUR   .72   FINISH
MATERIALS &
TYPE 10 NAME "Lacustrine" COLOR 23 PATTERN -1031 &
TYPE 20 NAME "Fine Sand" COLOR 12 PATTERN -1030 &
TYPE 50 NAME "Fine Sand South" COLOR 3 PATTERN -1034 &
TYPE 60 NAME "Coarse Sand South" COLOR 4 PATTERN -1033 &
TYPE 30 NAME "Coarse Sand" COLOR 27 PATTERN -1025 &
TYPE 40 NAME "Glacial Moraine1" COLOR 9 PATTERN -1035 &
TYPE 70 NAME "Fine Lacustrine" COLOR 5 PATTERN -1032 &
TYPE 80 NAME "Ponds" COLOR 6 PATTERN 0 &
TYPE 90 NAME "Glacial Moraine2" COLOR 10 PATTERN -1035 &
TYPE 95 NAME "Glacial Moraine3" COLOR 11 PATTERN -1035 &
TYPE 96 NAME "Glacial Moraine4" COLOR 13 PATTERN -1035 &
FINISH
!
COLOR &
NUMBER 27 HUE  150 LIGHT 60 SATUR 75 &
NUMBER 41 HUE  210 LIGHT 80 SATUR 100 &
NUMBER 47 HUE  150 LIGHT 80 SATUR 75 &
NUMBER 44 HUE  150 LIGHT 93 SATUR 75 &
NUMBER 24 HUE  0 LIGHT 90 SATUR 100 &
NUMBER 20 HUE  180 LIGHT 50 SATUR 100 &
NUMBER 76 HUE  120 LIGHT 85 SATUR 100 &
NUMBER 19 HUE  0 LIGHT 90 SATUR 100 &
NUMBER 21 HUE  280 LIGHT 80 SATUR 100 &
NUMBER 16 HUE  60 LIGHT 85 SATUR 100 &
NUMBER 17 HUE  210 LIGHT 70 SATUR 100 &
NUMBER 23 HUE  150 LIGHT 60 SATUR 65 &
NUMBER 45 HUE  120 LIGHT 85 SATUR 100 &
FINISH
BASEMAP mmr.map FINISH
WELLFILE CS4.WEL FINISH
OBSFILE CS4WT.OBS FINISH
QUIT
```

C-2. Well file

!WELL FILE INCLUDING ALL THE WELLS USED AS TARGETS FOR CALIBRATION AND THE !REMEDIATION WELLS

!

WELL TYPE

2 REMEDIATION

4 TARGETS

FINISH

!

!WELL ID, WELL ID FOR DISPLAY IN DYNPLOT, SITE, WELL TYPE, X, Y, GROUND !SURFACE ELEVATION, TOP OF SCREEN ELEVATION, BOTTOM OF SCREEN ELEVATION

!

"CS4MHW1","MH1","CS-4"2,16903,18955,91.43,127,142

"CS4MHW2","MH2","CS4",2,16847,18975,91.43,127,142

"CS4MHW3","MH3","CS4",2,16789,18992,93,127,142

"CS4MHW4","MH4","CS4",2,16733,19012,93.81,127,142

"CS4MHW5","MH5","CS4",2,16676,19030,94.15,127,142

"CS4MHW6","MH6","CS4",2,16619,19049,94.4,127,142

"CS4MHW7","MH7","CS4",2,16562,19067,94.25,127,142

"CS4MHW8","MH8","CS4",2,16505,19086,93.8,127,142

"CS4MHW9","MH9","CS4",2,16448,19105,93.43,127,142

"CS4MHW10","MH10","CS4",2,16391,19123,93.22,127,142

"CS4MHW11","MH11","CS4",2,16345,19160,93.21,127,142

"CS4MHW12","MH12","CS4",2,16276,19163,93.17,127,142

"CS4MHW13","MH13","CS4",2,16220,19179,93.44,127,142

"WT-1","WT-1","West-Cape",4,4387.14,11794.85,10,0,-5

"WT-2","WT-2","West-Cape",4,12673.47,51031.31,10,0,-5

"WT-3","WT-3","West-Cape",4,37159.28,51506.74,10,0,-5

"WT-4","WT-4","West-Cape",4,46266.51,54674.79,10,0,-5

"WT-5","WT-5","West-Cape",4,33255.82,47022.32,10,0,-5

"WT-6","WT-6","West-Cape",4,6390.23,39529.29,10,0,-5

"WT-7","WT-7","West-Cape",4,28775.31,39991.86,10,0,-5

"WT-8","WT-8","West-Cape",4,38963.85,39714.09,10,0,-5

"WT-9","WT-9","West-Cape",4,22297.52,36148.45,10,0,-5

"WT-10","WT-10","Study-area",4,24572.6,36023.23,10,0,-5

"WT-11","WT-11","West-Cape",4,27910.3,34087.22,10,0,-5

"WT-12","WT-12","West-Cape",4,30229.02,36823.2,10,0,-5

"WT-13","WT-13","West-Cape",4,8120.433,32357.76,10,0,-5

"WT-14","WT-14","West-Cape",4,10295.57,31355.13,10,0,-5

"WT-15","WT-15","Study-area",4,13271.61,31269.19,10,0,-5

"WT-16","WT-16","Study-area",4,15727.59,31192.24,10,0,-5

"WT-17","WT-17","Study-area",4,16522.69,32999.54,10,0,-5

"WT-18","WT-18","Study-area",4,19224.36,34042.07,10,0,-5

"WT-19","WT-19","Study-area",4,23796.36,34114.13,10,0,-5

"WT-20","WT-20","Study-area",4,25411.84,30528.7,10,0,-5

"WT-21","WT-21","West-Cape",4,28473.1,29341.06,10,0,-5

"WT-22","WT-22","West-Cape",4,33590.06,28077.12,10,0,-5
"WT-23","WT-23","West-Cape",4,10037.26,29677.7,10,0,-5
"WT-24","WT-24","Study-area",4,13840.84,30377.24,10,0,-5
"WT-25","WT-25","Study-area",4,14008.03,29328.41,10,0,-5
"WT-26","WT-26","Study-area",4,14824.34,29070.6,10,0,-5
"WT-28","WT-28","Study-area",4,15246.19,28409.48,10,0,-5
"WT-29","WT-29","Study-area",4,15009.94,27550.86,10,0,-5
"WT-30","WT-30","Study-area",4,13489.56,26644.15,10,0,-5
"WT-31","WT-31","West-Cape",4,7106.703,26686.77,10,0,-5
"WT-32","WT-32","Study-area",4,11557.09,26814.26,10,0,-5
"WT-33","WT-33","Study-area",4,15035.51,26118.74,10,0,-5
"WT-34","WT-34","Study-area",4,17483.41,26055.99,10,0,-5
"WT-35","WT-35","Study-area",4,22776.48,28207.01,10,0,-5
"WT-36","WT-36","Study-area",4,20813.14,24624.97,10,0,-5
"WT-37","WT-37","West-Cape",4,5814.297,22900.7,10,0,-5
"WT-38","WT-38","Study-area",4,13358.65,24228.05,10,0,-5
"WT-39","WT-39","Study-area",4,15874.34,23722.49,10,0,-5
"WT-40","WT-40","Study-area",4,17662.88,23330.96,10,0,-5
"WT-41","WT-41","Study-area",4,22153.35,22747.35,10,0,-5
"WT-42","WT-42","Study-area",4,25470.1,26077,10,0,-5
"WT-43","WT-43","Study-area",4,25346.38,22909.84,10,0,-5
"WT-44","WT-44","West-Cape",4,29220.54,24482.62,10,0,-5
"WT-45","WT-45","West-Cape",4,30386.07,22657.36,10,0,-5
"WT-46","WT-46","Study-area",4,20948.41,21297.83,10,0,-5
"WT-47","WT-47","Study-area",4,17225.08,20358.15,10,0,-5
"WT-48","WT-48","Study-area",4,26451.29,20220.55,10,0,-5
"WT-49","WT-49","Study-area",4,17980.1,19203.16,10,0,-5
"WT-50","WT-50","Study-area",4,23537.23,18880.99,10,0,-5
"WT-51","WT-51","Study-area",4,23477.75,18420.6,10,0,-5
"WT-52","WT-52","Study-area",4,21622.98,17877.85,10,0,-5
"WT-53","WT-53","West-Cape",4,28847.71,19609.95,10,0,-5
"WT-54","WT-54","West-Cape",4,30415.19,19391.84,10,0,-5
"WT-55","WT-55","West-Cape",4,33850.9,19623.23,10,0,-5
"WT-56","WT-56","Study-area",4,15828.19,18241.51,10,0,-5
"WT-57","WT-57","Study-area",4,18642.99,17489.78,10,0,-5
"WT-58","WT-58","Study-area",4,22709.2,17725.01,10,0,-5
"WT-59","WT-59","Study-area",4,20791.15,16047.38,10,0,-5
"WT-60","WT-60","Study-area",4,23942.88,16236.68,10,0,-5
"WT-61","WT-61","Study-area",4,25809.57,16401.44,10,0,-5
"WT-62","WT-62","Study-area",4,26180.71,15923.78,10,0,-5
"WT-63","WT-63","Study-area",4,26556.41,15463.89,10,0,-5
"WT-64","WT-64","Study-area",4,18320.01,15509.81,10,0,-5
"WT-65","WT-65","Study-area",4,22064.67,15291.32,10,0,-5
"WT-66","WT-66","Study-area",4,23691.86,14297.6,10,0,-5
"WT-67","WT-67","Study-area",4,14461.82,12928.42,10,0,-5
"WT-68","WT-68","Study-area",4,18224.73,13339.51,10,0,-5
"WT-69","WT-69","Study-area",4,21223.32,12641.44,10,0,-5
"WT-70","WT-70","Study-area",4,18618.73,12472.31,10,0,-5
"WT-71","WT-71","West-Cape",4,18214.41,11440.39,10,0,-5

"WT-72","WT-72","West-Cape",4,16633.97,10598.7,10,0,-5
"WT-73","WT-73","West-Cape",4,19729.45,9448.173,10,0,-5
"WT-74","WT-74","West-Cape",4,20209.89,9619.373,10,0,-5
"WT-75","WT-75","West-Cape",4,23383.66,10002.59,10,0,-5
"WT-76","WT-76","West-Cape",4,26416.27,10440.75,10,0,-5
"WT-77","WT-77","West-Cape",4,15018.2,9041.107,10,0,-5
"WT-78","WT-78","West-Cape",4,16053.61,8997.077,10,0,-5
"WT-79","WT-79","West-Cape",4,16020.56,8325.323,10,0,-5
"WT-80","WT-80","West-Cape",4,15334.75,7583.017,10,0,-5
"WT-81","WT-81","West-Cape",4,26026.92,8697.523,10,0,-5
"WT-82","WT-82","West-Cape",4,22373.51,7281.757,10,0,-5
"WT-83","WT-83","West-Cape",4,869.41,7349.173,10,0,-5
"WT-84","WT-84","West-Cape",4,10071.37,7739.45,10,0,-5
"WT-85","WT-85","West-Cape",4,11275.48,6929.937,10,0,-5
"WT-86","WT-86","West-Cape",4,18835.51,6680.463,10,0,-5
"WT-87","WT-87","West-Cape",4,18197.25,5805.983,10,0,-5
"WT-88","WT-88","West-Cape",4,20571.37,5403.797,10,0,-5
"WT-89","WT-89","West-Cape",4,27350.17,6115.59,10,0,-5
"WT-90","WT-90","West-Cape",4,25086.88,4539.743,10,0,-5
"WT-91","WT-91","West-Cape",4,27345.43,3939.703,10,0,-5
"WT-92","WT-92","West-Cape",4,27008.33,1950.713,10,0,-5
"WT-93","WT-93","West-Cape",4,5983.773,4570.093,10,0,-5
"WT-94","WT-94","West-Cape",4,15437.47,4925.15,10,0,-5
"WT-95","WT-95","West-Cape",4,14901,4048.703,10,0,-5
"WT-96","WT-96","West-Cape",4,13414.03,3139.063,10,0,-5
"WT-97","WT-97","West-Cape",4,16829.41,2637.27,10,0,-5
"WT-98","WT-98","West-Cape",4,15844.1,1913.047,10,0,-5
"WT-99","WT-99","West-Cape",4,310.6033,2798.987,10,0,-5
"WT-100","WT-100","West-Cape",4,1935.22,2439.97,10,0,-5
"WT-101","WT-101","West-Cape",4,10333.16,-182.213,10,0,-5
"WT-102","WT-102","West-Cape",4,15084.66,7.306667,10,0,-5
"WT-103","WT-103","West-Cape",4,17785.16,-1156.64,10,0,-5
"WT-104","WT-104","West-Cape",4,20507.71,-1294.38,10,0,-5
"WT-105","WT-105","West-Cape",4,21074.93,1109.72,10,0,-5

C-3. Observation file with water table elevations

!OBSERVATION FILE CONTAINING THE HEAD DATA FROM THE 106 WELLS USED AS !TARGETS

```
!
PARAMETERS
head UNITS ft
FINISH
!
DATE GROUPS
1/1/93
12/1/93
FINISH
!
"WT-1","head","3/3/93",18.64
"WT-2","head","3/3/93",45.69
"WT-3","head","3/3/93",58.04
"WT-4","head","3/3/93",39.35
"WT-5","head","3/3/93",64.89
"WT-6","head","3/3/93",23.58
"WT-7","head","3/3/93",69.35
"WT-8","head","3/3/93",64.53
"WT-9","head","3/3/93",64.37
"WT-10","head","3/3/93",66.07
"WT-11","head","3/3/93",67.63
"WT-12","head","3/3/93",68.24
"WT-13","head","3/3/93",38.19
"WT-14","head","3/3/93",45.33
"WT-15","head","3/3/93",52.73
"WT-16","head","3/3/93",57.27
"WT-17","head","3/3/93",59.04
"WT-18","head","3/3/93",62
"WT-19","head","3/3/93",64.99
"WT-20","head","3/3/93",62.04
"WT-21","head","3/3/93",61.85
"WT-22","head","3/3/93",59.13
"WT-23","head","3/3/93",43.92
"WT-24","head","3/3/93",54.33
"WT-25","head","3/3/93",53.14
"WT-26","head","3/3/93",51.14
"WT-28","head","3/3/93",54.61
"WT-29","head","3/3/93",53.67
"WT-30","head","3/3/93",50.38
"WT-31","head","3/3/93",29.97
"WT-32","head","3/3/93",47.26
"WT-33","head","3/3/93",52.63
"WT-34","head","3/3/93",54.92
"WT-35","head","3/3/93",59.57
```

"WT-36","head","3/3/93",54.77
"WT-37","head","3/3/93",27.09
"WT-38","head","3/3/93",47.83
"WT-39","head","3/3/93",50.49
"WT-40","head","3/3/93",51.19
"WT-41","head","3/3/93",51.6
"WT-42","head","3/3/93",57.44
"WT-43","head","3/3/93",51.54
"WT-44","head","3/3/93",54.98
"WT-45","head","3/3/93",50.06
"WT-46","head","3/3/93",49
"WT-47","head","3/3/93",46.05
"WT-48","head","3/3/93",45.07
"WT-49","head","3/3/93",44.65
"WT-50","head","3/3/93",44.99
"WT-51","head","3/3/93",44.87
"WT-52","head","3/3/93",44.12
"WT-53","head","3/3/93",41.6
"WT-54","head","3/3/93",38.52
"WT-55","head","3/3/93",37.52
"WT-56","head","3/3/93",41.76
"WT-57","head","3/3/93",42.22
"WT-58","head","3/3/93",44.38
"WT-59","head","3/3/93",41.89
"WT-60","head","3/3/93",42.95
"WT-61","head","3/3/93",44.22
"WT-62","head","3/3/93",41.06
"WT-63","head","3/3/93",39.78
"WT-64","head","3/3/93",38.75
"WT-65","head","3/3/93",41.2
"WT-66","head","3/3/93",40.32
"WT-67","head","3/3/93",32.24
"WT-68","head","3/3/93",36.06
"WT-69","head","3/3/93",37.41
"WT-70","head","3/3/93",35.47
"WT-71","head","3/3/93",33.74
"WT-72","head","3/3/93",31.14
"WT-73","head","3/3/93",31.46
"WT-74","head","3/3/93",32.09
"WT-75","head","3/3/93",33.26
"WT-76","head","3/3/93",34.27
"WT-77","head","3/3/93",25.14
"WT-78","head","3/3/93",26.57
"WT-79","head","3/3/93",25.21
"WT-80","head","3/3/93",22.66
"WT-81","head","3/3/93",30.58
"WT-82","head","3/3/93",28.6
"WT-83","head","3/3/93",12.67
"WT-84","head","3/3/93",23.57

"WT-85","head","3/3/93",21.92
"WT-86","head","3/3/93",24.36
"WT-87","head","3/3/93",21.04
"WT-88","head","3/3/93",22.56
"WT-89","head","3/3/93",20.31
"WT-90","head","3/3/93",20.5
"WT-91","head","3/3/93",15.9
"WT-92","head","3/3/93",7.08
"WT-93","head","3/3/93",15.76
"WT-94","head","3/3/93",17.49
"WT-95","head","3/3/93",15.51
"WT-96","head","3/3/93",15.59
"WT-97","head","3/3/93",13.35
"WT-98","head","3/3/93",11.7
"WT-99","head","3/3/93",10.17
"WT-100","head","3/3/93",12.23
"WT-101","head","3/3/93",12.27
"WT-102","head","3/3/93",7.59
"WT-103","head","3/3/93",5.74
"WT-104","head","3/3/93",5.45
"WT-105","head","3/3/93",13.18
"WT-106","head","3/3/93",6

C-4. Command files

! COMMAND FILE TO ASSIGN ONE-DIMENSIONAL ELEMENTS TO THE WELLS
!
! RESTORE THE FILE WITH ZERO FLUXES AND NO ONED ELEMENTS
REST CS-4.SAV
ONED 122 NODE 1276 1276 LEVEL 6 7
ONED 122 NODE 1276 1276 LEVEL 7 8
ONED 122 NODE 142 142 LEVEL 6 7
ONED 122 NODE 142 142 LEVEL 7 8
ONED 122 NODE 1270 1270 LEVEL 6 7
ONED 122 NODE 1270 1270 LEVEL 7 8
ONED 122 NODE 143 143 LEVEL 6 7
ONED 122 NODE 143 143 LEVEL 7 8
ONED 122 NODE 1271 1271 LEVEL 6 7
ONED 122 NODE 1271 1271 LEVEL 7 8
ONED 122 NODE 1269 1269 LEVEL 6 7
ONED 122 NODE 1269 1269 LEVEL 7 8
ONED 122 NODE 1272 1272 LEVEL 6 7
ONED 122 NODE 1272 1272 LEVEL 7 8
ONED 122 NODE 99 99 LEVEL 6 7
ONED 122 NODE 99 99 LEVEL 7 8
ONED 122 NODE 1275 1275 LEVEL 6 7

```
ONED 122 NODE 1275 1275 LEVEL 7 8
ONED 122 NODE 100 100 LEVEL 6 7
ONED 122 NODE 100 100 LEVEL 7 8
ONED 122 NODE 1274 1274 LEVEL 6 7
ONED 122 NODE 1274 1274 LEVEL 7 8
ONED 122 NODE 101 101 LEVEL 6 7
ONED 122 NODE 101 101 LEVEL 7 8
ONED 122 NODE 1273 1274 LEVEL 6 7
ONED 122 NODE 1273 1274 LEVEL 7 8
XCFI
```

!COMMAND FILE USED TO ASSIGN PUMPING RATES TO THE WELLS OF THE WELL FENCE
!EACH WELL HAS A ONE-DIMENTIONAL ELEMENT ASSOCIATED
!VALUES OF PUMPING RATE IN CUBIC FEET PER DAY

```
!
! PUMPRATE.CFI
! COMMAND FILE TO ASSIGN FLUXES TO THE WELLS
! RESTORE THE FILE WITH ZERO FLUXES
REST C.SAV
! well 13
FLUX NODE 142 LEVEL 8 VALUE 0
FLUX NODE 142 LEVEL 7 6 VALUE 0
! well 12
FLUX NODE 1270 LEVEL 6 7 VALUE 0
FLUX NODE 1270 LEVEL 8 VALUE 0
! well 11
FLUX NODE 143 LEVEL 6 7 VALUE0
FLUX NODE 143 LEVEL 8 VALUE 0
! well 10
FLUX NODE 1271 LEVEL 6 7 VALUE -1
FLUX NODE 1271 LEVEL 8 VALUE -5775.3
! well 9
FLUX NODE 1269 LEVEL 6 7 VALUE 0
FLUX NODE 1269 LEVEL 8 VALUE 0
! well 8
FLUX NODE 1272 LEVEL 6 7 VALUE 0
FLUX NODE 1272 LEVEL 8 VALUE 0
! well 7
FLUX NODE 1276 LEVEL 6 7 VALUE -1
FLUX NODE 1276 LEVEL 8 VALUE -5775.3
! well 6
FLUX NODE 99 LEVEL 6 7 VALUE 0
FLUX NODE 99 LEVEL 8 VALUE 0
! well 5
FLUX NODE 1275 LEVEL 6 7 VALUE 0
```

```
FLUX NODE 1275 LEVEL 8 VALUE 0
! well 4
FLUX NODE 100 LEVEL 6 7 VALUE -1
FLUX NODE 100 LEVEL 8 VALUE -5775.3
! well 3
FLUX NODE 1274 LEVEL 6 7 VALUE 0
FLUX NODE 1274 LEVEL 8 VALUE 0
! well 2
FLUX NODE 101 LEVEL 6 7 VALUE 0
FLUX NODE 101 LEVEL 8 VALUE 0
! well 1
FLUX NODE 1273 LEVEL 6 7 VALUE 0
FLUX NODE 1273 LEVEL 8 VALUE 0
!run flow model
GOTI
!save flow model
SAVE C3.SAV
XCFI
```

C-5. Particle tracking command files

```
!COMMAND FILE TO HORIZONTAL PARTICLE TRACKING, CAPTURE CURVE
!SIMULATIONS
!
! restore the Dynflow file
REST C3a210.SAV
! create an output file
OUTP SAVE t.OUT FORM
! read the transport property file
DPRO READ CURVES.PRP
! specify the type of run (in this case, with dispersion)
XDISP
! take into account scale dependent dispersion
! SDDS
! starting time (units: days)
WEIGH 1000.
TIME 0.
! time step (units: days)
DT 20.
PART 2
16454.978,21181.167,-20
PART 3
16511.988,21162.467,-20
PART 4
16568.998,21143.767,-20
PART 5
16626.008,21125.067,-20
```

```
PART 6
16683.018,21106.367,-20
PART 7
16740.028,21087.667,-20
PART 8
16797.038,21068.967,-20
PART 9
16854.048,21050.267,-20
PART 10
16911.058,21031.567,-20
PART 11
16968.068,21012.867,-20
PART 12
17025.078,20994.167,-20
PART 13
17082.088,20975.467,-20
PART 14
17139.098,20956.767,-20
PART 15
17196.108,20938.067,-20
PART 16
17253.118,20919.367,-20
PART 17
17310.128,20900.667,-20
PART 18
17367.138,20881.967,-20
PART 19
17424.148,20863.267,-20
PART 20
17481.158,20844.567,-20
PART 21
17538.168,20825.867,-20
PART 22
17595.178,20807.167,-20
PART 23
17652.188,20788.467,-20
PART 24
17709.198,20769.767,-20
PART 25
17766.208,20751.067,-20
PART 26
17823.218,20732.367,-20
PART 27
17880.228,20713.667,-20
RESU 50 SAVE t.RES
GOTI 5000
! finish
XRES
END
```

```
!COMMAND FILEFOR CROSS-SECTIONAL PARTICLE TRACKING, CAPTURE
CURVE !SIMULATIONS. RESULTS OF THIS SIMULATION TO BE USED WITH THE
"PLOT !STARTING POINTS" DYNPLOT OPTION
!
!NOTE: SAMPLE OF THE ORIGINAL FILE. ONLY TWO LEVELS OF PARTICLES
!ARE SHOWN (Z = 42 AND Z = -80)
!
! restore the Dynflow file
REST C13.SAV
! create an output file
OUTP SAVE XS13.OUT FORM
! read the transport property file
DPRO READ CURVES.PRP
! specify the type of run (in this case, with dispersion)
XDISP
! take into account scale dependent dispersion
! SDDS
! starting time (units: days)
WEIGH 1000.
TIME 0.
! time step (units: days)
DT 20.
PART 1
17937.24,20694.97,42
PART 3
16568.998,21143.767,42
PART 4
16626.008,21125.067,42
PART 5
16683.018,21106.367,42
PART 6
16740.028,21087.667,42
PART 7
16797.038,21068.967,42
PART 8
16854.048,21050.267,42
PART 9
16911.058,21031.567,42
PART 10
16968.068,21012.867,42
PART 11
17025.078,20994.167,42
PART 12
17082.088,20975.467,42
PART 13
17139.098,20956.767,42
PART 14
17196.108,20938.067,42
PART 15
```

17253.118,20919.367,42
PART 16
17310.128,20900.667,42
PART 17
17367.138,20881.967,42
PART 18
17424.148,20863.267,42
PART 19
17481.158,20844.567,42
PART 20
17538.168,20825.867,42
PART 21
17595.178,20807.167,42
PART 22
17652.188,20788.467,42
PART 23
17709.198,20769.767,42
PART 24
17766.208,20751.067,42
PART 25
17823.218,20732.367,42
PART 26
17880.228,20713.667,42
!
PART 263
17937.24,20694.97,-80
PART 264
16568.998,21143.767,-80
PART 265
16626.008,21125.067,-80
PART 266
16683.018,21106.367,-80
PART 267
16740.028,21087.667,-80
PART 268
16797.038,21068.967,-80
PART 269
16854.048,21050.267,-80
PART 270
16911.058,21031.567,-80
PART 271
16968.068,21012.867,-80
PART 272
17025.078,20994.167,-80
PART 273
17082.088,20975.467,-80
PART 274
17139.098,20956.767,-80
PART 275

17196.108,20938.067,-80
PART 276
17253.118,20919.367,-80
PART 278
17310.128,20900.667,-80
PART 279
17367.138,20881.967,-80
PART 280
17424.148,20863.267,-80
PART 281
17481.158,20844.567,-80
PART 282
17538.168,20825.867,-80
PART 283
17595.178,20807.167,-80
PART 284
17652.188,20788.467,-80
PART 285
17709.198,20769.767,-80
PART 286
17766.208,20751.067,-80
PART 287
17823.218,20732.367,-80
PART 289
17880.228,20713.667,-80
RESU 50 SAVE XS13.RES
GOTI 5000
! finish
XRES
END